3. CRITERIA FOR FA AND DDT LIMITS*

3.1 Introduction

The processes following weak ignition in a combustible mixture can result in generation of a variety of different combustion regimes ranging from slow flames to detonations. Different combustion regimes occur because of the intrinsic ability of combustion waves to accelerate and to undergo transition to detonation. Fast combustion modes that resulted from FA and DDT can be extremely destructive. Thus from the practical point of view, it is important to predict the type of combustion regimes that can be developed under certain initial and boundary conditions.

Detailed description of all processes following weak ignition in a combustible mixture is extremely difficult at present. This is due to complicated interactions of compressible flow, turbulence, and chemical reactions, which should be described at high spatial and temporal resolution. In this situation, much effort has been focused on development of criteria for FA and DDT. These criteria are aimed at description of initial and boundary conditions under which flame acceleration and DDT can be expected. An overview of criteria that can be used to evaluate possibility of FA and DDT is presented in this chapter.

3.2 Criteria for FA

3.2.1 Buoyancy Limits

3.2.1.1 Downward/upward flame propagation limits.

Buoyancy effects essentially limit the ability of flame acceleration for mixtures that are close to flammability limits. If ignition occurs in a mixture, which is in between upward and downward propagation limits (in hydrogen-air mixtures at normal initial conditions these are 4 vol % and 8 vol %), incomplete combustion is observed. Buoyancy lifts the flame ball upward as it expands, and hence only a fraction of the total volume of the mixture is burned. The turbulence is able to enhance the completeness of combustion, but no chance exists for effective flame acceleration under these conditions. Thus a comparison of the composition of the mixture with that for the download propagation limit gives an indication of the possibility of flame acceleration.

3.2.1.2 Froude number

Froude number Fr is a dimensionless parameter, which determines the influence of natural convection on flame shape and properties

$$Fr = v^2/2gR \,, \tag{3.1}$$

where v is visible flame speed, g is gravitational acceleration, and R is flame radius. The critical value of the Froude number is estimated to be $Fr^* = 0.11$ [3.1]. For $Fr < Fr^*$, buoyancy dominates the process of expansion of combustion products. Under these conditions, the most effective mechanism of flame acceleration (feedback between the flame flow produced and the flame itself) does not work. The critical Froude number may be used as a criterion for the possibility of flame acceleration.

---

* Dr. Sergei B. Dorofeev is the lead author for this chapter.

For laminar H_2-air flames of 1 m in radius, values of Froude number are 0.05 and 0.16 for mixtures of 9% and 10% H_2 in air, assuming $v = \sigma S_L$ (where σ is ratio of densities of reactants and products, and S_L is laminar flame speed). This gives a reasonable estimate that flames with H_2 concentration of less than 9.5% and $R > 1$ m should be significantly affected by buoyancy. It should be noted that estimates of the buoyancy effect that make use of Froude number are not as direct and easy as it seems. Such estimates are reliable only for small-enough flame kernels, which can be considered as laminar. In other cases, values of visible flame speed, v, are required, which depend on the actual combustion regime.

3.2.2 Effects of Mixture Reactivity and Scale (σ - Criterion)

Unlike the buoyancy-driven flames, deflagrations dominated by the product expansion provide favourable conditions for flame acceleration. If such a possibility exists, it is important to estimate whether the flame is able to accelerate under given conditions resulting in fast turbulent combustion regimes (such as ‘sonic’ or ‘choked’ flames) and, possibly, in the transition to detonation, or the flame acceleration is inefficient ending at a benign combustion and even flame quenching.

An important fundamental problem that should be solved to provide a foundation for such predictions is an adequate description of the mutual affect of scale and mixture properties on the resulting combustion mode. The influence of various factors, including scale, on the turbulent flame propagation and flame acceleration phenomenon was studied extensively (see e. g., [3.2-3.7]). Turbulent velocity correlations have been suggested in References [3.5 to 3.7] and in other studies, which include intrinsically the effect of scale. However, quantitative criteria for flame acceleration are difficult to formulate on the basis of these correlations because they require that a current level of turbulence to be known in all phases of the process.

A series of tests was recently conducted to systematically study the effects of scale and mixture properties on the behaviour of turbulent flames in obstructed areas [3.8, 3.9]. A set of dimensionless parameters was chosen that could influence the flame-flow-flame feedback in obstructed areas. These parameters are defined by the intrinsic length, time and velocity scales of the combustion processes, and by mixture properties:

$$L_T/\delta,\ \sigma,\ S_L/c_{sr},\ S_L/c_{sp},\ \gamma_r,\ Le, \text{ and } \beta\ , \tag{3.2}$$

where L_T is the integral length scale of turbulence, δ is the laminar flame thickness, σ is the ratio of densities of reactants and products (expansion ratio), S_L is the laminar flame speed, c_{sr} and c_{sp} are the sound speeds in reactants and products, γ_r is the specific heat ratio in reactants, Le is the Lewis number, $\beta = E_a(T_b - T_u)/(RT_b^2)$ is the Zeldovich number, E_a is the effective activation energy, T_u is the initial, and T_b is the maximum flame temperature.

In obstructed areas, the integral length scale of turbulence is defined mainly by geometrical configuration [3.10]. Other parameters in Equation (3.2) are defined by mixture properties. The parameters in Equation (3.2), thus, can be considered as those defining a priori a *potential* for flame acceleration.

The experiments described in References [3.8 and 3.9] were focused on the effect of these parameters. Three tubes (174, 350, and 520 mm id) and explosion channel (80 mm x 80 mm cross-section) were used in the tests. Different mixtures were chosen in order to provide (1) a wide range of the scaling parameters and (2) combinations with similar values of the parameters at different scales.

It was found that under certain conditions the flame accelerates effectively in explosion channels, resulting in fast supersonic (in a laboratory framework) regimes of propagation such as choked flames and detonations. Another option was ineffective flame acceleration resulting in relatively slow, subsonic regimes of propagation. Some examples are presented in Figures. 3.2.2-1 to 3.2.2-3. For slow combustion regimes, the maximum speed of flame propagation appeared to increase with scale. Despite this effect, a very significant difference in the maximum propagation speeds and corresponding levels of overpressures was observed between slow and fast regimes for all scales. This significant difference allows us to define a criterion for flame acceleration that is based on the corresponding critical conditions in channels with obstacles.

Experimental results [3.8, 3.9] showed that parameters L/δ and σ were the most important ones among all the sets (3.2) in defining flame acceleration rate. At the same time, the type (slow or fast) of final regime of flame propagation at sufficiently large scale was found to depend mainly on the value of mixture expansion ratio σ. In view of this observation, it was suggested that all mixtures may be divided into "weak" and "strong". Flame acceleration and development of fast combustion regimes are possible in strong mixtures under favourable conditions at sufficiently large scale. Flame acceleration in weak mixtures is inefficient, even under favourable conditions. A criterion for flame acceleration was suggested in Reference [3.10] as a requirement of a large-enough value of σ:

$$\sigma > \sigma^*(\beta, Le)\ , \qquad (3.3)$$

where σ^* is the critical value, which is expected to be function of β and Le.

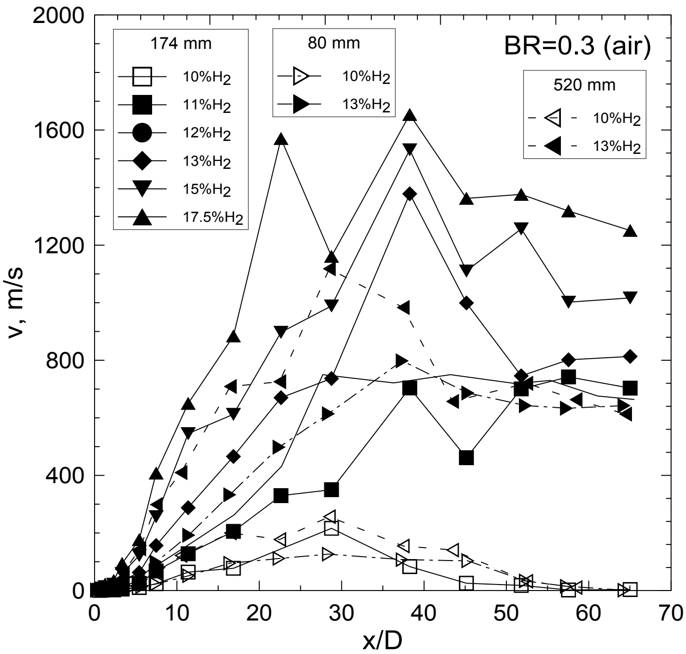

Figure 3.2.2-1 Visible speeds of flame propagation versus reduced distance along tubes (*D* - tube diameter) for lean hydrogen-air mixtures. Blockage ratio = 0.3; obstacle spacing is equal to *D*. Solid points represent fast combustion regimes (choked flames and quasi-detonations); empty points represent slow combustion regimes.

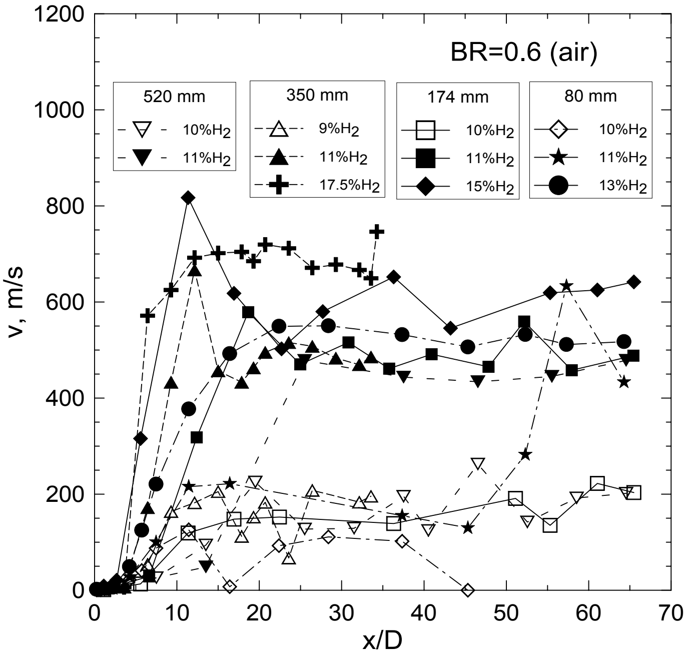

Figure 3.2.2-2 Visible speeds of flame propagation versus reduced distance along for lean hydrogen-air mixtures. Blockage ratio = 0.6. Solid points show fast combustion regimes (choked flames); empty points show slow combustion regimes.

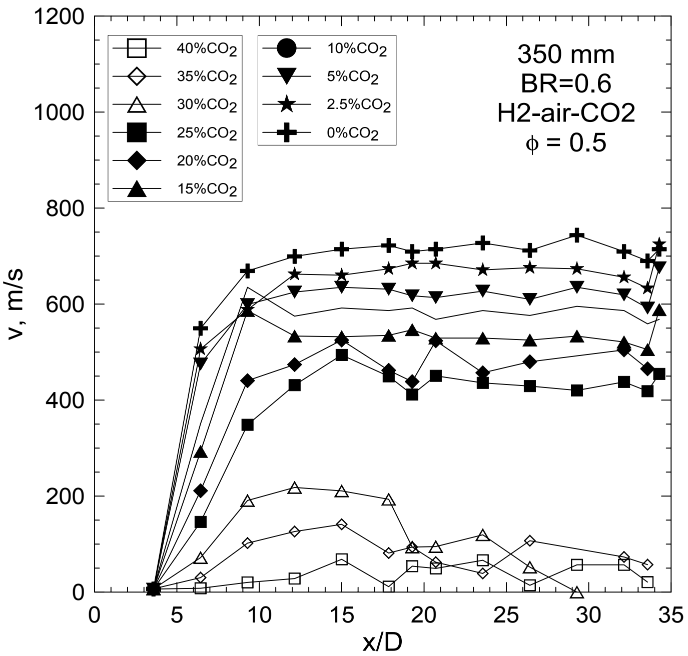

Figure 3.2.2-3 Visible speeds of flame propagation versus reduced distance along the tube for lean hydrogen-air mixtures (equivalence ratio $\phi = 0.5$) diluted with CO_2. Blockage ratio = 0.6. Solid points show fast combustion regimes (choked flames); empty points show slow combustion regimes.

3.2.3 Experimental Correlations for FA Criterion

A large amount of experimental data on turbulent flame acceleration is available at conditions representative of nuclear safety. In this section, these data are considered.

Experiments were conducted in the High-Temperature Combustion Facility (HTCF) facility at the Brookhaven National Laboratory (BNL) to study flame acceleration and DDT in hydrogen-air and hydrogen-air-steam mixtures with different hydrogen and steam concentrations. The experiments were performed without venting and with 5.1% venting at initial mixture temperatures up to 650K [3.11]. The HTCF is 21.3 m long and has an internal diameter of 27.3 cm. Periodic orifice plates were installed down the length of the entire detonation tube. The orifice plates have an outer diameter of 27.3 cm, an inner diameter of 20.6 cm, and a spacing of 1 tube diameter.

Experiments were conducted at the Sandia National Laboratories (SNL) with hydrogen-air-steam and hydrogen-air mixtures in the Heated Detonation Tube (HDT) to determine the region of benign combustion (between the flammability limits and the DDT limits) [3.12]. The HDT is 12 m long and has internal diameter of 43 cm. Obstacles were used with 30% blockage ratio annular rings, and alternate rings and disks of 60% blockage ratio. The initial conditions were 383 K and 1 or 3 atm pressure.

RUT facility tests were performed at Russian Research Centre “Kurchatov Institute” (RRC KI0 with hydrogen-air mixtures with and without steam dilution in a complex geometry [3.13, 3.14]. The first part of the facility was a channel of 2.5 x 2.3-m cross-section and 34.6 m long; the second part was a canyon of 6 x 2.5-m cross-section and 10.5 m long, and the third one was a channel of 2.5 x 2.3-m cross-section and 20 m long. Twelve concrete obstacles were placed along the first channel with a spacing of 2.5 m (blockage ratios were 0.3 and 0.6). Initial temperature in tests with steam was close to 375 K. Initial pressure in all the tests was 1 atm.

FLAME facility data were obtained at the Sandia National Laboratories in a study of FA and DDT of hydrogen-air mixtures [3.15]. FLAME is a large (30.5 m long) rectangular channel that has an interior width of 1.83 m and a height of 2.44 m. The blockage ratio was 0.0 (no obstacles) or 0.33 in the tests. Initial conditions were normal in these tests.

FZK experiments [3.9] were performed in a 35-cm-diameter, 12-m-long length with equidistant rings as obstacles (blockage ratio was 0.6 spacing was 35cm). Flame acceleration was studied in hydrogen-air mixtures and in hydrogen-oxygen (2:1) mixture, diluted with nitrogen, argon, helium and CO_2. Experiments were conducted under normal initial conditions.

CHANNEL, DRIVER, and TORPEDO experiments provided data on turbulent flame propagation regimes in obstructed areas at different scales [3.8, 3.9]. Blockage ratios ranged from 0.1 to 0.9. Distances between obstacles were equal to the transverse size of each tube for all these facilities. Mixture compositions were varied in the tests. Experiments were conducted under normal conditions. The CHANNEL facility is a tube with a square cross-section of 80 mm × 80 mm and 5.28-m length. Rectangular obstacles were mounted along upper and bottom plates. Different hydrogen-air mixtures and stoichiometric hydrogen-oxygen, diluted by argon or helium were used in these tests. The DRIVER facility is a detonation tube of 174 mm id and approximately 12-m length. Hydrogen-air mixtures and stoichiometric hydrogen-oxygen mixtures diluted with nitrogen, argon, or helium were used in this facility. The TORPEDO facility is a 520-mm tube of 30.3-m length. Hydrogen-air mixtures and stoichiometric hydrogen-oxygen, diluted by helium were used in these tests.

Results of the analyses [3.10] are presented in Figures 3.2.3-1 to 3.2.3-6. Data points are marked with labels given in Table 3.2.3-1. Black points correspond to fast combustion regimes, and light gray points to slow combustion regimes.

Table 3.2.3-1 Experimental data used in correlations for flame acceleration criterion

Data source	**Label**	**Blockage ratio BR**	**Tube or channel size L, mm**	**Initial temperatur e T, K**	**Mixture type**	**Equivalence ratio ϕ**
HTCF-BNL [3.11]	b1	0.43	273	300	H_2/air	<1
HTCF-BNL [3.11]	b2	0.43	273	500	H_2/air	<1
HTCF-BNL [3.11]	b3	0.43	273	650	H_2/air	<1
HTCF-BNL [3.11]	b4	0.43	273	400	H_2/air/H_2O	<1
HTCF-BNL [3.11]	b5	0.43	273	500	H_2/air/H_2O	<1
HTCF-BNL [3.11]	b6	0.43	273	650	H_2/air/H_2O	<1
CHANNEL-RRCKI [3.9]	c1	0.1	80	293	H_2/air	<1; >1
CHANNEL-RRCKI [3.9]	c2	0.3	80	293	H_2/air	<1; >1
CHANNEL-RRCKI [3.9]	c3	0.6	80	293	H_2/air	<1; >1
CHANNEL-RRCKI [3.9]	c4	0.9	80	293	H_2/air	<1; >1
CHANNEL-RRCKI [3.9]	c5	0.6	80	293	H_2/O_2/He	1
CHANNEL-RRCKI [3.9]	c6	0.6	80	293	H_2/O_2/Ar	1
DRIVER-RRCKI [3.9]	d1	0.09	174	293	H_2/air	<1; >1
DRIVER-RRCKI [3.9]	d2	0.3	174	293	H_2/air	<1; >1
DRIVER-RRCKI [3.9]	d3	0.6	174	293	H_2/air	<1; >1
DRIVER-RRCKI [3.9]	d4	0.9	174	293	H_2/air	<1; >1
DRIVER-RRCKI [3.9]	d5	0.09	174	293	H_2/O_2/N_2	1
DRIVER-RRCKI [3.9]	d6	0.3	174	293	H_2/O_2/N_2	1
DRIVER-RRCKI [3.9]	d7	0.6	174	293	H_2/O_2/N_2	1
DRIVER-RRCKI [3.9]	d8	0.9	174	293	H_2/O_2/N_2	1
DRIVER-RRCKI [3.9]	e1	0.09	174	293	H_2/O_2/He	1
DRIVER-RRCKI [3.9]	e2	0.3	174	293	H_2/O_2/He	1
DRIVER-RRCKI [3.9]	e3	0.6	174	293	H_2/O_2/He	1
DRIVER-RRCKI [3.9]	e5	0.09	174	293	H_2/O_2/Ar	1
DRIVER-RRCKI [3.9]	e6	0.3	174	293	H_2/O_2/Ar	1
DRIVER-RRCKI [3.9]	e7	0.6	174	293	H_2/O_2/Ar	1
FLAME-SNL [3.15]	f1	0.33	1830	293	H_2/air	<1
FLAME-SNL [3.15]	f2	0	1830	293	H_2/air	<1
FZK [3.9]	g1	0.6	350	293	H_2/air	<1; >1
FZK [3.9]	g2	0.6	350	293	H_2/O_2/N_2	1
FZK [3.9]	g3	0.6	350	293	H_2/O_2/He	1
FZK [3.9]	g4	0.6	350	293	H_2/O_2/Ar	1
FZK [3.9]	g5	0.6	350	293	H_2/O_2/CO_2	1
FZK [3.9]	g6	0.6	350	293	H_2/air/CO_2	.5
FZK [3.9]	g7	0.6	350	293	H_2/air/CO_2	1
FZK [3.9]	g8	0.6	350	293	H_2/air/CO_2	2
FZK [3.9]	g9	0.6	350	293	H_2/air/CO_2	4

continued . . .

Table 3.2.3-1 (concluded)

Data source	Label	Blockage ratio BR	Tube or channel size L, mm	Initial temperature T, K	Mixture type	Equivalence ratio ϕ
RUT-RRCKI [3.13]	r1	0.6	2250	293	H_2/air	<1
RUT-RRCKI [3.13]	r2	0.3	2250	293	H_2/air	<1
RUT-RRCKI [3.13]	r3	0	2250	293	H_2/air	<1
RUT-RRCKI [3.14]	r4	0.3	2250	375	H_2/air/H_2O	≤1
HDT-SNL [3.12]	s1	0.6	406	383	H_2/air	>1
HDT-SNL [3.12]	s2	0.3	406	383	H_2/air/H_2O	>1
TORPEDO-RRCKI [3.9]	t1	0.6	520	293	H_2/air	<1; >1
TORPEDO-RRCKI [3.9]	t2	0.6	520	293	H_2/O_2/He	1
TORPEDO-RRCKI [3.9]	t3	0.3	520	293	H_2/air	<1; >1
TORPEDO-RRCKI [3.9]	t4	0.1	520	293	H_2/air	<1; >1

The plot of σ-values versus initial temperature is shown in Figure 3.2.3-1. It is seen that the border between fast and slow flames in terms of σ goes down with initial temperature. In fact, such a behaviour should be expected. The mixtures are characterized by the intrinsic temperature scale - parameter *Ea/R*. In the dimensionless form, the rigorous parameter is the Zeldovich number $\beta = Ea(T_b - T_u)/RT_b^2$. Qualitatively, the influence of initial temperature on effectiveness of the flame acceleration is connected with the increase of the effect of local turbulent mixing on suppression of burning rate at high β-values. Such a general effect, however, is expected to be influenced by a local behaviour of a flame element that is stretched and curved by turbulent motions.

The Zeldovich number is known to play an important role in the stability of stretched flames in a combination with the Lewis number [3.16]. Normal burning rate of stretched flames U_n relative to burned mixture may be expressed by

$$U_n/U_L-1 = -Ma_b\, \delta/U_L \cdot (1/A \cdot dA/dt)\ , \qquad (3.3)$$

where U_L is the laminar flame speed relative to burned mixture, A is the elementary area of the flame front, and Ma_b is the Markstein number defined relative to burned mixture.

The value of $1/A \cdot dA/dt$ represents the flame stretch, which in highly turbulent flow is due to turbulence. The value of the Markstein number, Ma_b, determines the effect of stretch on variations of local burning velocities. For two reactant mixtures with a single-step reaction the Ma_b is estimated as [3.16]:

$$Ma_b = \frac{\sigma}{\sigma-1}\left(\ln\sigma + \frac{\beta(Le-1)}{2(\sigma-1)}\right)\int_0^{\sigma-1}\frac{\ln(1+x)dx}{x}\ , \qquad (3.4)$$

where x is dummy variable of integration. The combination $\beta(Le-1)$ defines the value and even the sign of Ma_b. At large negative values of $\beta(Le-1)$, $Ma_b < 0$ and the flame stretch results in a local increase of burning velocity. With $Ma_b > 0$, the flame stretch tends to decrease the burning velocity and can result in flame quench.

The combination $\beta(Le\text{-}1)$ is also the defining parameter for thermal-diffusion flame instability. The stability boundary corresponds to $\beta(Le\text{-}1) = -2$. Flames are stable with $\beta(Le\text{-}1) > -2$, and unstable with $\beta(Le\text{-}1) < -2$. These speculations show that parameter $\beta(Le\text{-}1)$ is expected to be important in correlations of experimental data.

Figure 3.2.3-2 shows combustion regimes in $(\sigma$ - $\beta(Le\text{-}1))$ plot. The value $\beta(Le\text{-}1)$ = -2 indeed appeared as a threshold value. With $\beta(Le\text{-}1)$ < - 2 the borderline between slow and fast combustion regimes changes with $\beta(Le\text{-}1)$ in the range σ^* = 2 - 3.75. With $\beta(Le\text{-}1)$ > -2, which corresponds to thermal-diffusely stable flames, an abrupt change of limiting values of σ is observed. Values of σ ranges from 3.5 to 4.0 for $\beta(Le\text{-}1)$ > -2. A similar picture is seen in the $(\sigma$ - $Ma_b)$ plot presented in Figure 3.2.3-3. Threshold value here corresponds to $Ma_b = 0$.

Data of Figures 3.2.3-2 and 3.2.3-3 suggest that correlations with other parameters should be made separately for mixtures with $\beta(Le\text{-}1)$ < -2 and with $\beta(Le\text{-}1)$ > -2. For stable flames with $\beta(Le\text{-}1)$ > -2, these correlations are presented in Figures 3.2.3-4 and 3.2.3-5. Critical σ-values for effective flame acceleration do not depend significantly on scale ratio L/δ (Figure 3.2.3-4 and on Zeldovich number β (Figure 3.2.3-5). For unstable flames with $\beta(Le\text{-}1)$ < -2, critical σ-values can be considered to be a function of Zeldovich number β (Figure 3.2.3-6).

Experimental correlations presented in this section permit us to suggest the following <u>necessary</u> conditions for development of fast combustion regimes [3.10].

$$\sigma > (3.5 \div 4), \quad \text{for mixtures with } \beta(Le - 1) > -2\ ; \tag{3.5}$$

$$\sigma > \sigma^*(\beta), \quad \text{for mixtures with } \beta(Le - 1) < -2\ , \tag{3.6}$$

where the function $\sigma^*(\beta)$ is given by the correlation shown in Figure 3.2.3-6. These conditions are expressed in terms of mixture properties and give the possibility to divide mixtures into “strong” and “weak”, depending on their ability to support effective flame acceleration under favourable geometrical conditions.

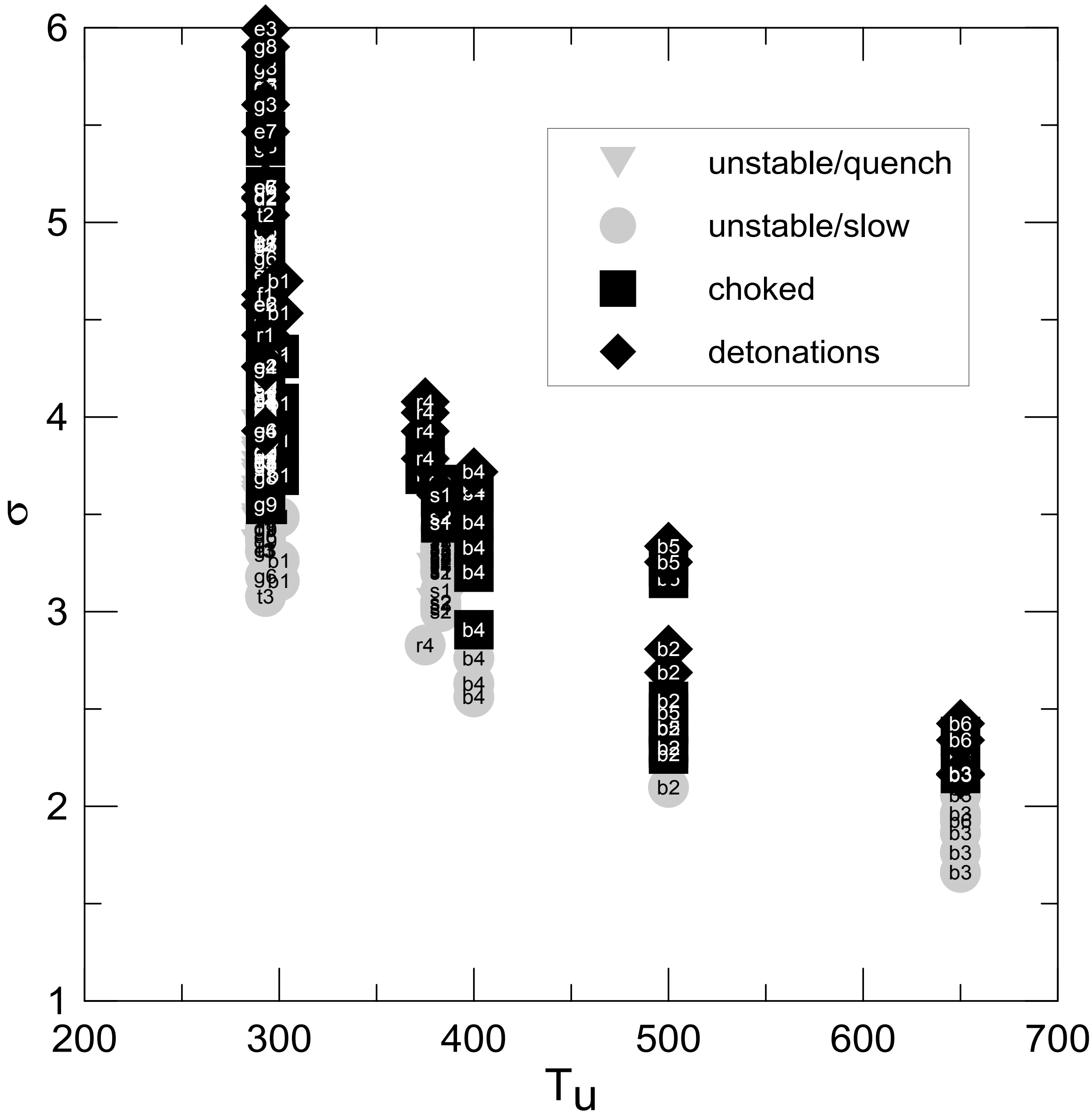

Figure 3.2.3-1 Resulting combustion regime as a function of expansion ratio σ and initial temperature T_u. Black points show fast combustion regimes, and gray points show slow combustion regimes.

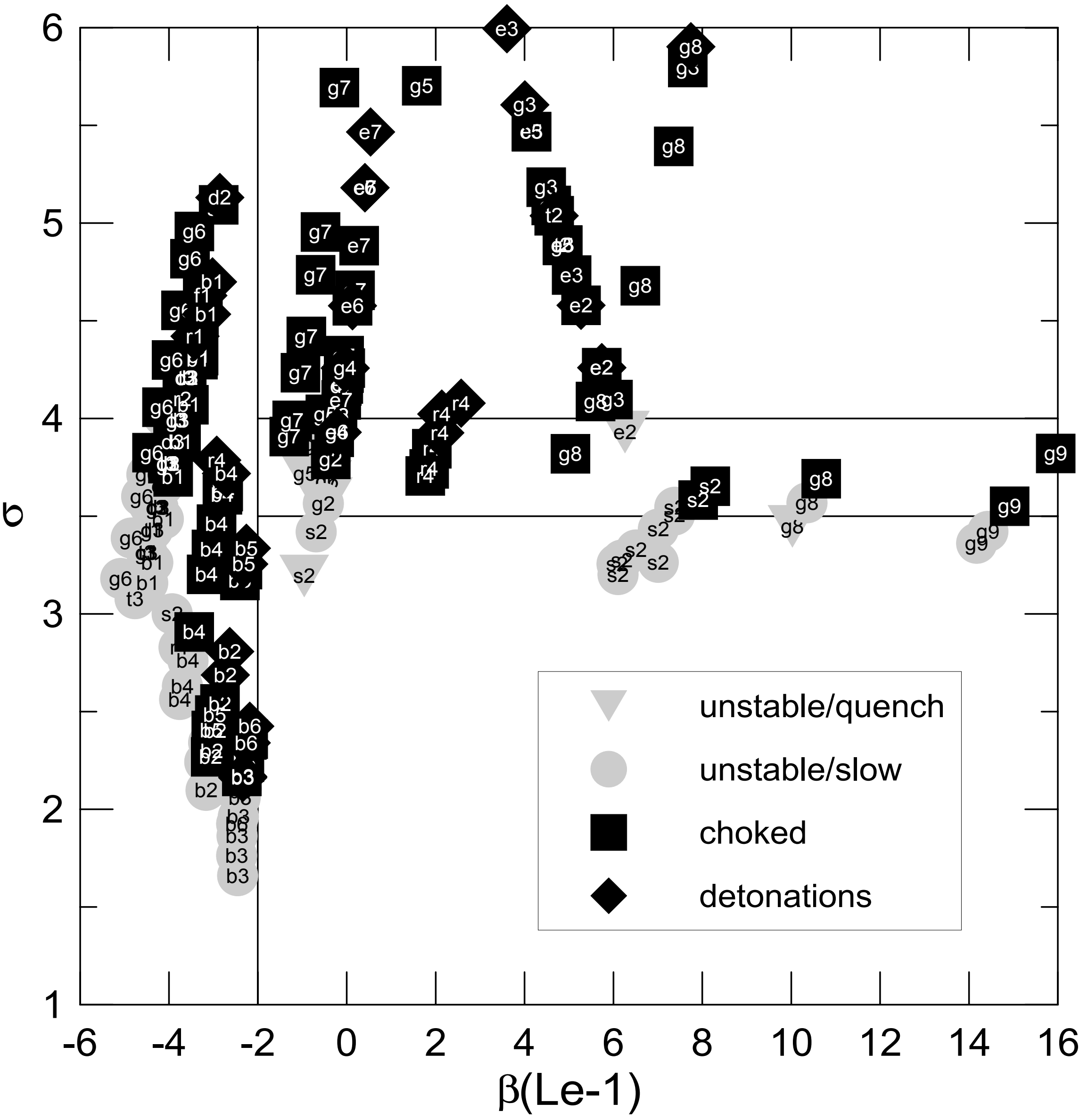

Figure 3.2.3-2 Resulting combustion regime as a function of expansion ratio σ and $\beta(Le - 1)$. Black points represent fast combustion regimes, and gray points represent slow combustion regimes.

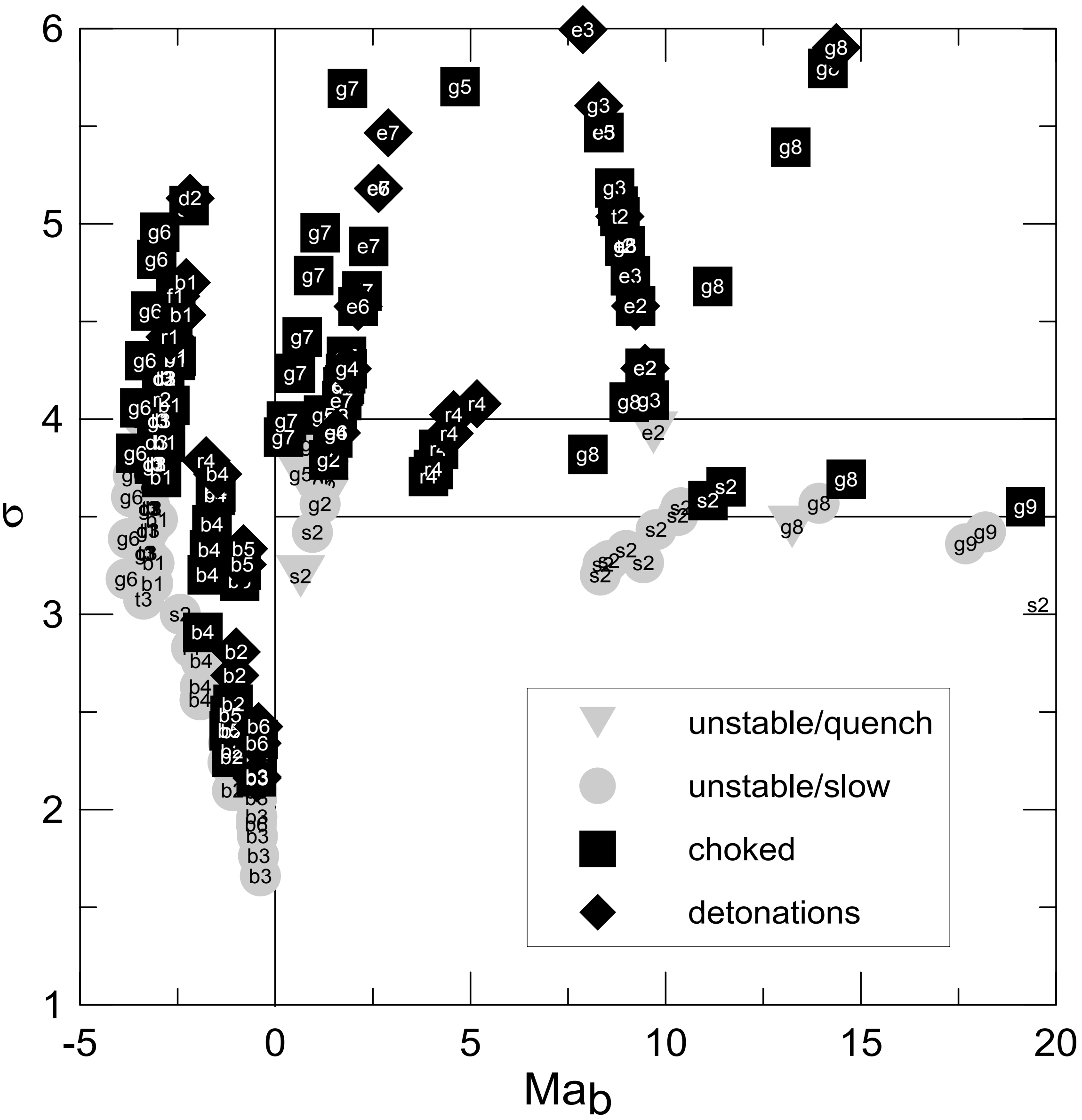

Figure 3.2.3-3 Resulting combustion regime as a function of expansion ratio σ and Ma_b. Black points represent fast combustion regimes, and gray points represent slow combustion regimes.

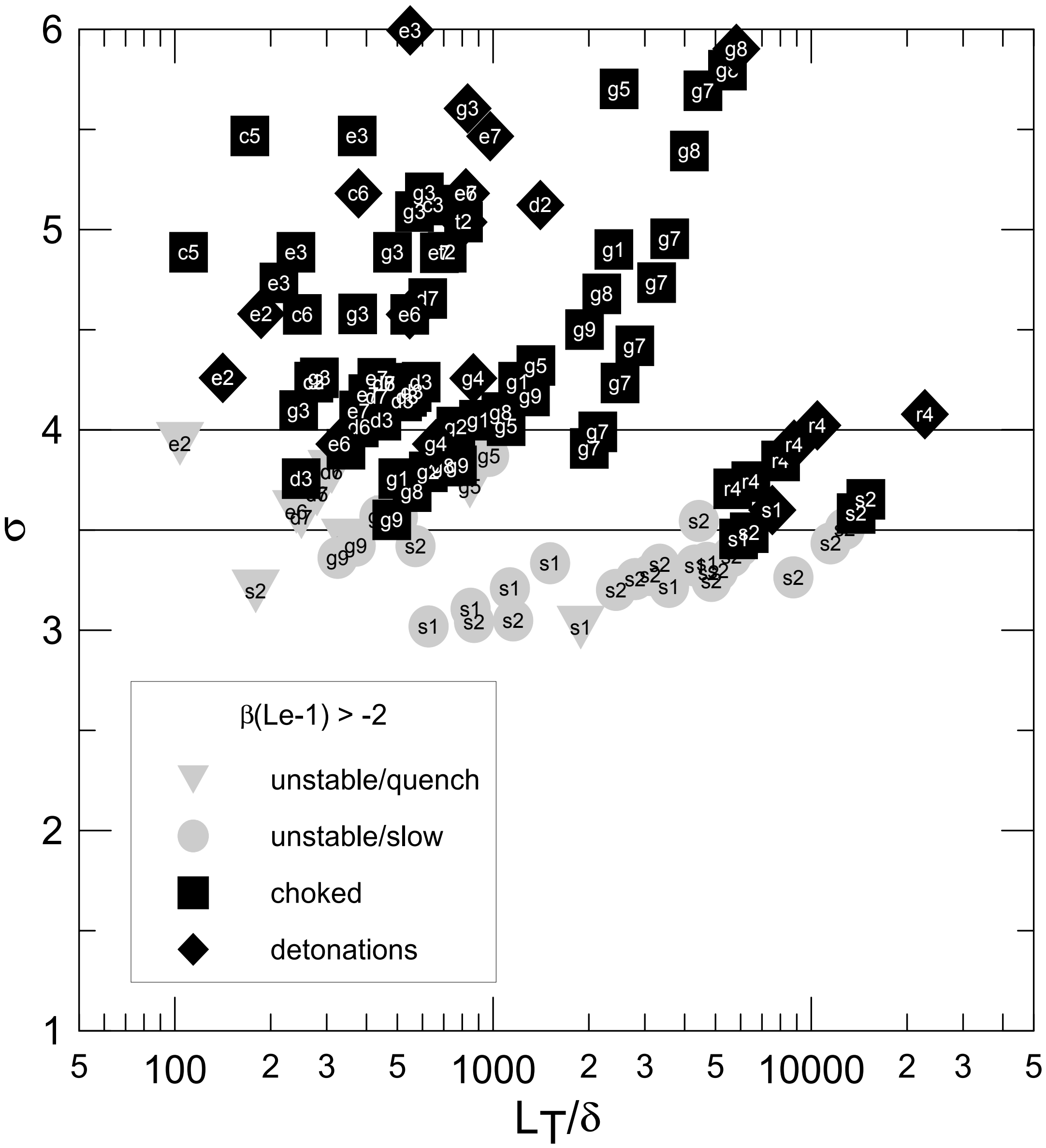

Figure 3.2.3-4 Resulting combustion regime as a function of expansion ratio *σ* and scale ratio *L/δ* for mixtures with *β(Le - 1)* > -2. Black points represent fast combustion regimes, and gray points represent slow combustion regimes.

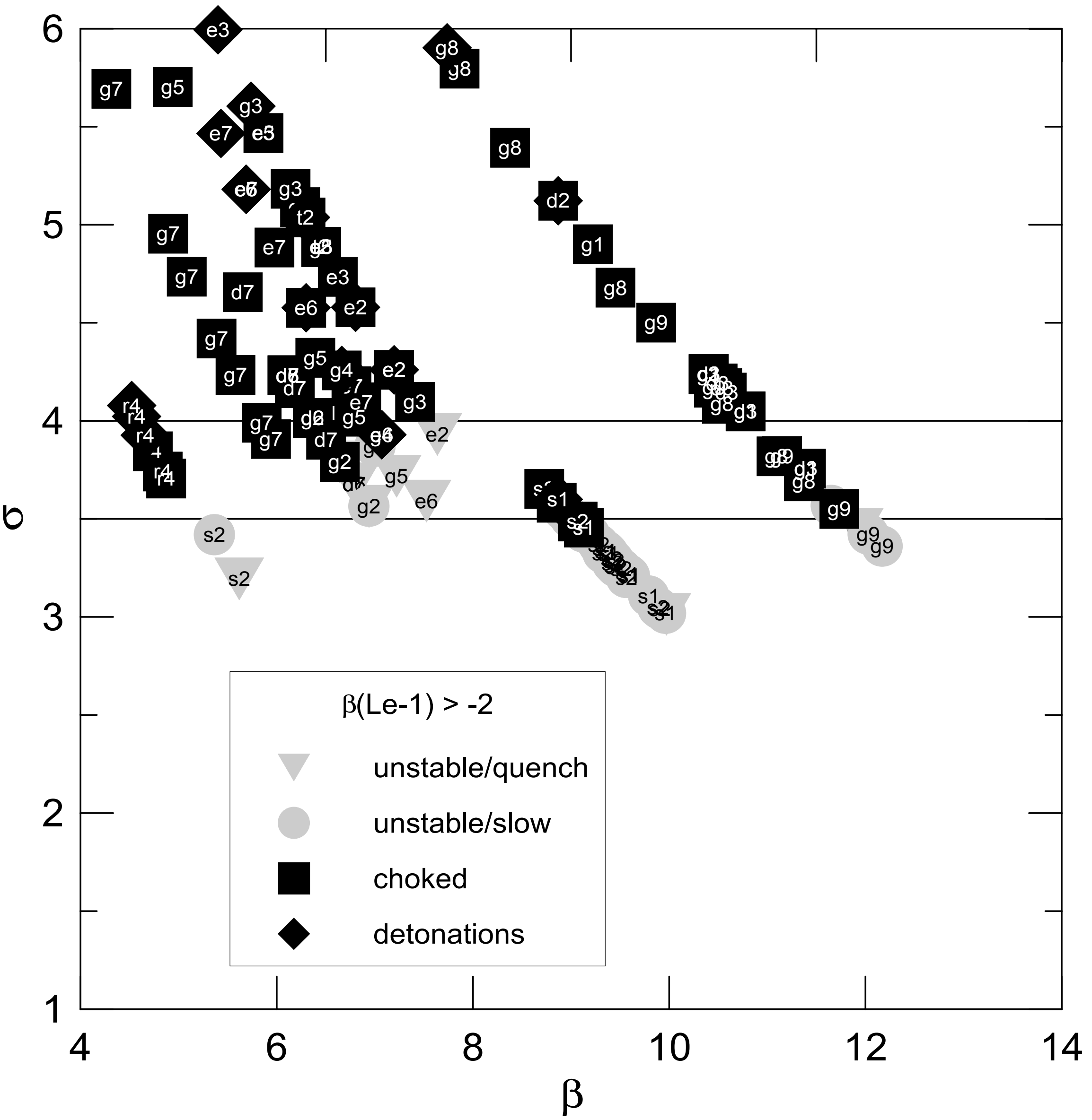

Figure 3.2.3-5 Resulting combustion regime as a function of expansion ratio σ and Zeldovich number β for mixtures with $\beta(Le - 1) > -2$. Black points represent fast combustion regimes. and gray points represent slow combustion regimes.

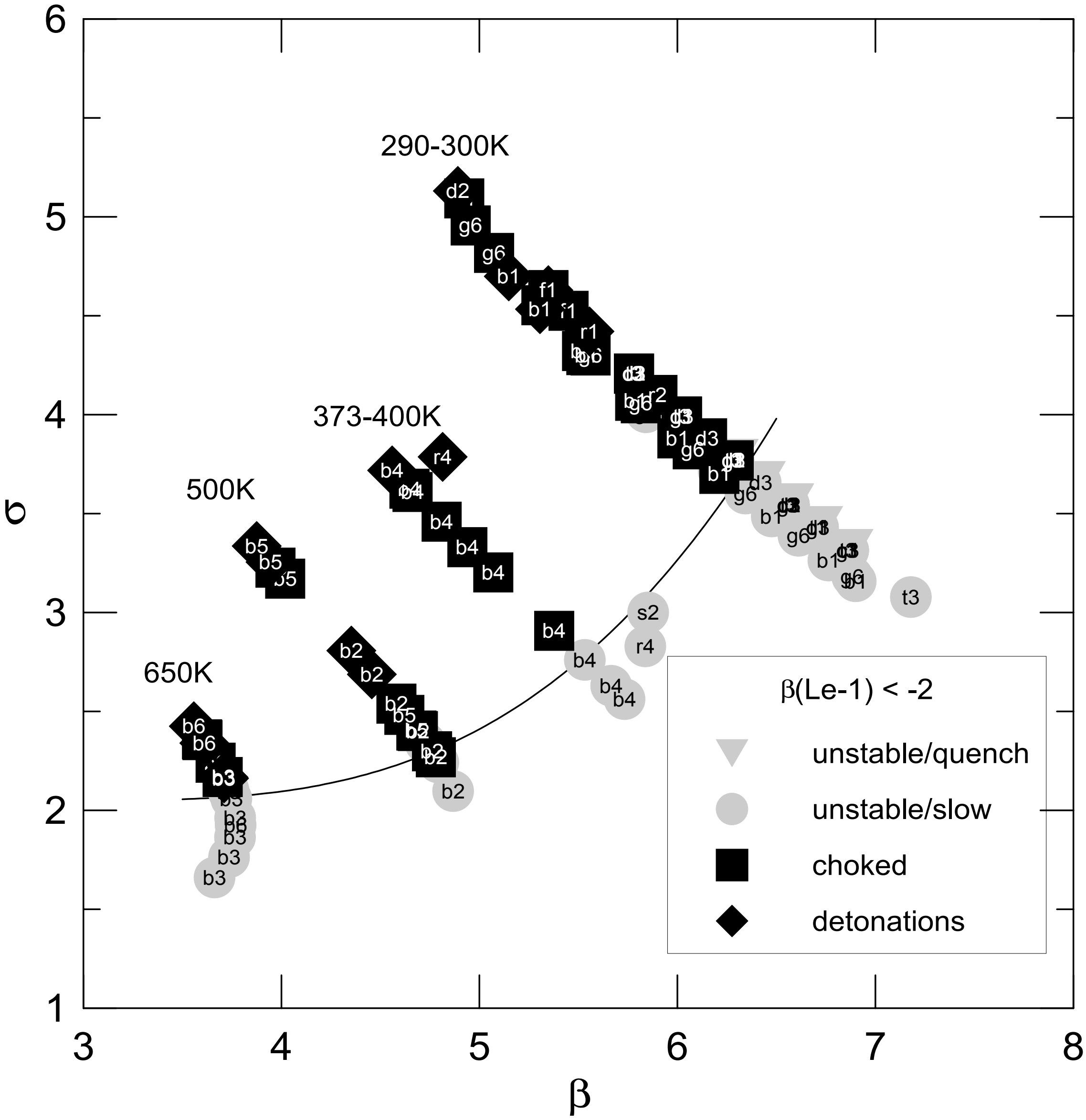

Figure 3.2.3-6 Resulting combustion regime as a function of expansion ratio σ and Zeldovich number β for mixtures with $\beta(Le - 1) < -2$. Black points represent fast combustion regimes, and gray points represent slow combustion regimes. Groups of points are marked with values of initial temperatures for hydrogen-air-steam mixtures.

3.2.4 Applications of σ - Criterion and Corresponding Uncertainties

To apply the criteria stated in Equations (3.5) and (3.6), values of β and *Le* are required for each particular mixture. First of all, the value of $\beta(Le\text{-}1)$ should be estimated. For mixtures typical of containment atmospheres (hydrogen-air-steam) such estimates [3.10] suggest that H_2-lean mixtures are characterized by $\beta(Le - 1) < -2$ and H_2-rich and stoichiometric ones by $\beta(Le - 1) > -2$. Mixtures close to stoichiometry on the lean side with equivalence ratio ϕ from 0.7 to 1.0 (depending on initial temperature and steam concentration) are at the border $\beta(Le - 1) = -2$.

Thus for H_2-rich and stoichiometric hydrogen-air-steam mixtures, the condition expressed in Equation (3.6) should be applied to estimate limits of effective flame acceleration. For H_2-lean hydrogen-air-steam mixtures, limits for effective flame acceleration are expected to depend on β, and, hence, on initial temperature.

To calculate β, the values of effective activation energy *Ea* and T_b in addition to T_u are required. Thermodynamic calculations provide data on T_b for each particular mixture (equilibrium temperature of combustion products at constant pressure). Effective activation energy *Ea* can be estimated from dependence of laminar flame speed on T_b. For lean hydrogen-air-steam mixtures, such estimates give an average value of $Ea/R \approx 9800$ K (for rich mixtures $Ea/R \approx 17700$ K) [3.10]. These estimates and a correlation shown in Figure 3.2.3-6 provide data for determination of flame acceleration limits in terms of mixture compositions.

There are some uncertainties connected with estimations of flame acceleration limits. First of all, it should be stressed once more that the criteria expressed in Equations (3.5) and (3.6) represent necessary but not sufficient conditions for effective flame acceleration. Other requirements should be met as well so that the flame propagation can result in formation of fast combustion regimes. The most important of them are the requirements of a large-enough scale (flame propagation distance) and favourable geometry (obstructions) for effective flame acceleration.

Another type of uncertainty is connected with a spread of critical σ-values. For rich mixtures, it is given by the range from 3.5 to 4.0 for σ^*. It should also be noted that no experimental data are available for rich hydrogen-air-steam mixtures at $T_u > 383$ K. Additional experiments are required to evaluate the limit expressed in Equation (3.6) for rich mixtures at $T_u > 383$ K.

A considerable spread in limiting σ-values ($3.5 \div 4.0$) may be connected with an influence of additional parameters on effectiveness of flame acceleration. In particular, the laminar flame Mach number S_L/c_{sr} may play a role. An accurate estimation of the possible influence of this parameter is difficult because no reliable data on S_L are available for some of mixture compositions. In view of this, definition of critical conditions in terms of σ (even taking into account the spread of critical values) should be considered as more reliable because σ-values are only given by thermodynamic mixture properties.

For lean mixtures, the error of limiting σ-values (Figure 3.2.3-6) can be estimated as ±4%, which results, for example, in the σ^*-range from 2.7 to 2.9 for $\beta \approx 5.5$ ($T_u \approx 400$ K). If hydrogen-air-steam mixtures are considered without additional components or dilution (e. g., CO_2, N_2, CO, etc.), the unavoidable uncertainty connected with determination of *Ea* (and, hence, β) can be eliminated by using limiting $\sigma^*(T_u)$-values from Figure 3.2.3-1 instead of those from Figure 3.2.3-6. In other cases, the critical condition in form of $\sigma^*(\beta)$ is preferable, and uncertainty in β-value should be taken into account.

A third type of uncertainty is connected with a border between stable and unstable flames $\beta(Le - 1) = -2$. The exact location of this border (in terms of the mixture composition under given initial conditions) is difficult to define because of inevitable errors in determination of *Le* and β. What is also unclear is how sharp the difference is in limiting conditions for mixtures that are close to this stability boundary. No experimental data are available for mixtures with $\beta(Le-1)$ from -2.2 to -1.3 in Figures 3.2.4-1 to -6. Additional analysis and, probably, experiments are necessary to clarify the critical conditions for mixtures with equivalence ratios ϕ in the range from 0.7 to 1.0.

Limits of flame acceleration for hydrogen-air-steam mixtures at T = 375 K and p = 1 atm and corresponding uncertainties are shown as an example in Figure 3.2.4-1. The limits are presented using hydrogen concentration in a dry mixture (H_2(dry) = $H_2/(H_2$+air), vol %) and steam concentration (vol %) as variables.

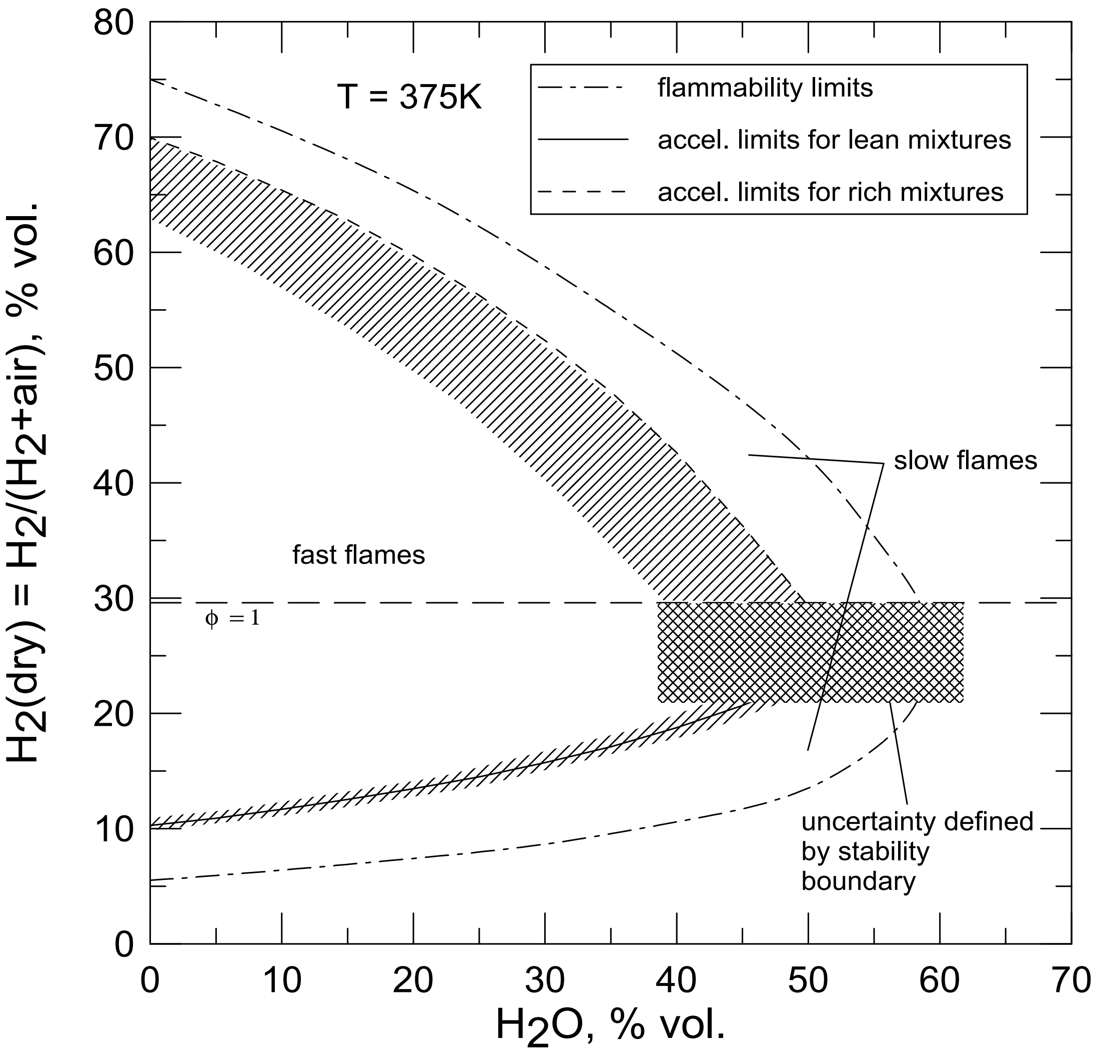

Figure 3.2.4-1 Limits of flame acceleration for hydrogen-air-steam mixtures at T = 375 K and p = 1 atm. Ranges of uncertainties are shown by shadow areas.

The uncertainties discussed above can be taken into account by using conservative estimates, that is, by using the minimum σ^*-values for each set of initial conditions. Additional experiments and analysis can help in narrowing the range of uncertainties in application of the σ-criterion.

3.3 Necessary Criteria for DDT

Useful practical information can be obtained if one addresses separately different phases of DDT, namely the creation of conditions for DDT (Phase 1) and the onset of detonations (Phase 2). For each of these phases, the necessary conditions may be formulated, which provide a number of DDT criteria for practical applications. These criteria give necessary but not sufficient conditions. If some or all of them are satisfied, it does not mean that detonation should certainly be initiated. There are probably other requirements that should also be met. However, if one of the necessary criteria is not satisfied, detonation should not be expected. This important point gives simple estimates from a conservative side for accident analysis.

3.3.1 Detonability Limits

The detonability limits of a reactive mixture are the critical conditions for the propagation of self-sustained detonation. The critical conditions denote both the initial and boundary conditions of the explosive mixture. If a self-sustained detonation propagation is not possible, DDT cannot be expected. In this view, the detonability limits can be considered as a “first level” of DDT criteria.

A detailed discussion of detonability limits can be found in several reviews (see e. g., [3.17-3.19]). Here we will just mention some important values. The limit for stable detonation propagation in a cylindrical smooth-walled tube (limiting tube diameter) is estimated to be $D^* = \lambda/\pi$. For wide planar channels with height H much smaller than the width W, the channel width should accommodate at least one detonation cell for stable detonation propagation $W^* = \lambda$.

3.3.2 Criteria for Phase 1 of DDT

It is generally considered that processes of DDT can be divided into two main phases. Phase 1 involves a variety of processes that create conditions for the onset of detonations. Phase 2 is the actual process of detonation formation – the onset of detonations. A number of requirements have been found that are necessary to provide conditions for DDT (Phase 1 of the process).

3.3.2.1 Fast flame requirement

It was shown that turbulent flames should accelerate to result in ‘choked’ or ‘sonic’ combustion regime to produce conditions for the onset of detonations [3.19, 3.20]. Flame speeds in laboratory flame are close to isobaric sound speeds in combustion products (about 500 to 1000 m/s) in this combustion regime. The results obtained recently show that no DDT was observed; indeed, in some cases a flame did not accelerate to a nearly choking regime. The necessary criterion may be formulated that the flame should be accelerated to result in a fast, nearly choking, combustion regime to make DDT possible. Thus the σ criterion for flame acceleration described in Section 3.2 can also used as one of the necessary conditions for DDT.

3.3.2.2 Critical flame Mach numbers

Because different initial conditions – in terms of mixture composition, temperature, and pressure— are relevant for nuclear safety, the definition of critical flame speeds in absolute values cannot be satisfactory. The flame Mach number (flame speed normalized by sound speed in uncompressed mixture) represents a parameter that is more relevant for a variety of initial conditions. The Mach number of choked flames is about 2. Recently, a series of tests was conducted [3.21] to determine the critical values of flame Mach numbers for DDT in a variety of hydrogen-air steam mixtures. The minimum value of 1.5 was found for the most-sensitive mixture used in the tests [3.21].

3.3.2.3 Minimum shock Mach numbers

The requirement of the development of a relatively fast combustion regime prior to DDT is connected with the necessary creation of a local explosion somewhere in the flow that includes flame brush and a system of shocks ahead of the flame. The faster the flame, the stronger the shocks generated, and consequently the more effective is the turbulent mixing of products and reactants, thereby promoting initiation of a localized explosion. One of the important mechanisms (but not the only one) that causes localized explosions to occur is connected with shock reflections from obstacles. Although mild ignitions in reflections are the intrinsic feature of propagating fast deflagration waves, strong ignitions can lead to formation of detonation wavelets, which in certain conditions can result in fully developed detonations.

To provide initiation of localized explosion in reflections, the flame should be able to generate a shock wave with some critical Mach number. A number of tests were made [3.22, 3.23] to determine the critical shock Mach numbers that are capable of giving strong ignition in reflections. The composition of mixtures and the configuration of reflectors were varied. More recently, critical shock Mach number experiments were conducted at a larger scale (FZK tube, 350 mm id) [3.24] compared with studies described in References [3.22 and 3.23].

The following conclusions can be made, to summarize the results of critical Mach number experiments in hydrogen-containing mixtures:

1. Shock (blast) waves with Mach numbers $M < 1.2$ cannot cause the secondary ignition being reflected from focusing surfaces and obstacles.

2. Shock (blast) waves with $1.2 < M < 1.4$ can cause secondary ignition in reflections from focusing surfaces and obstacles, thus favouring escalation of the explosion.

3. Shock (blast) waves with $M > 1.4$ can cause initiation of detonations in the vicinity of reflecting surfaces.

4. Scale affects the possibility of the initiation of detonation in shock-wave reflections. Usually, the critical Mach numbers for initiation of local detonations decrease as the scale increases.

No model is currently available that is able to adequately describe the mutual influence of shock strength, mixture properties, and scale on possibility of detonation initiation in reflections. The experimental data on detonation initiation in shock-wave reflections should help to develop and verify detailed models of DDT phenomena.

3.3.3 *Criteria for Onset of Detonations*

3.3.3.1 Minimum tube diameter criterion ($d > \lambda$)

A detailed study of DDT in tubes was conducted at McGill University [3.19, 3.20]. Flame acceleration and transition to detonation were studied in tubes having an internal diameter of 5 to 30 cm, and with orifice plates installed inside the tubes. Blockage ratio (BR), fuel type, and mixture composition were variables in these experiments. Detonation cell size, λ, was used to characterize the sensitivity of the mixture to detonation initiation. This means that different mixtures were compared on the basis of the value of the cell size. It was found that, for an optimum blockage ratio of BR = 0.43, a size of the unobstructed passage, d, of more than 1λ is necessary for transition to detonation. This criterion can be used as the necessary condition for DDT in obstructed channels. However, it is only applicable for very long channels, having a length of more than 10 to 20 times their width.

Long channels with or without obstacles are not typical of the geometry of containment buildings. A chain of connected compartments could principally represent a similar geometry. However, even for long channels, the critical value of *d* appeared to depend on obstacle configuration (see Table 3.3.3-1). The critical ratio d/λ increases with a decrease of obstacle spacing and with an increase of blockage ratio, BR. DDT is easier to achieve for a smaller BR and for a greater distance between obstacles. Variations of critical d/λ can be quite large, ranging from 0.8 to 5.1. Despite the obvious limitations of the criterion for long channels ($d > \lambda$), it gives an important indication of the effect of geometrical scale on the transition to detonation. The detonation cell size, λ, increases with changes of the mixture composition below and above stoichiometry. Consequently, the larger the scale the wider is the composition range for DDT.

Table 3.3.3-1 Critical conditions for DDT in channels and tubes having different configuration of obstacles

BR	Channel width *W*, mm	Channel height *H*, mm	Unobstructed passage *d*, mm	Obstacle spacing, mm	Maximum λ for DDT, mm	d/λ	Reference
0.43	16	57	31.6	50.56	8.8	3.6	[3.25]
0.43	16	57	31.6	101.12	11.7	2.7	[3.25]
0.43	50*		37.4	50	31	1.2	[3.26]
0.43	150*		114	150	100	1.1	[3.26]
0.43	300*		226	300	190	1.2	[3.26]
0.45	61.8	55.4	30	32.1	13	2.3	[3.27]
0.45	61.8	55.4	30	64.2	20	1.5	[3.27]
0.45	61.8	55.4	30	128.4	36	0.8	[3.27]
0.3	350*		293	525	220	1.3	[3.9]
0.6	350*		220	350	44	5.1	[3.9]

*) Tube diameter

3.3.3.2 Minimum scale requirement for onset of detonations

A number of studies focused on the analysis of the processes involved in the second phase of DDT – the onset of detonations. It was assumed that necessary conditions for generation of localized explosion (Phase 1) are met, and the process of the actual formation of a detonation wave was studied. It was shown that several factors can influence the process of detonation formation. First, a local distribution of mixture properties (auto-ignition delay time) in a sensitized region should provide coupling of chemical and gas dynamic processes that result in the formation of an explosion wave [3.28-3.30]. Second, this wave should survive propagating from a sensitized to an unpertubed mixture [3.31-3.34]. Finally, the explosion wave should be adjusted for a chemical length scale of the ambient mixture. The latter, naturally, gives a measure for the minimum size of the sensitized region, which is necessary for the formation of detonation.

Numerical and analytical studies were conducted to determine the minimum size of the sensitized region [3.31-3.35]. Critical conditions for detonation formation in a locally sensitized mixture were studied. A sensitized region was modelled by temperature distributions [3.31-3.33], addition of a fast reactive component [3.31-3.33], and mixed products and reactants [3.34]. The problem of the propagation of an explosion wave through reactivity gradients was also studied analytically as a separate problem [3.35].

The main results of these studies are summarized here: the minimum size of a sensitized region is required for the onset of a detonation; this size depends on the properties of the mixture surrounding the sensitized region; and a characteristic length scale for this process is of the order of 10λ, in terms of detonation cell width, λ, of the unperturbed mixture. Some details of the detonation formation process may influence the minimum size for detonation onset. A decrease of the volumetric energy content in the sensitized region (e. g., for temperature non-uniformities), results in the minimum size increase. In the opposite case of the detonation onset in a locally pre-compressed region (e. g., for auto-ignition from shock reflections), detonation onset is facilitated. In cases of detonation formation as an expanding wave (e. g., spherical symmetry), the minimum size was found to be increased because of curvature effects. A combination of the above factors is typical for DDT events. It is hardly possible, thus, to define a universal criterion for the onset of detonations. However, an engineering estimate for practical applications has been suggested [3.13, 3.31-3.33], assuming that a detonation is developed initially as a planar wave, volumetric energy content is uniform, and typical fuel-air mixtures are considered. With these assumptions, the minimum macroscopic size of sensitized mixture for detonation onset was estimated to be about 7λ.

The results of numerical studies described above were obtained using some types of one-dimensional (1D) models for detonation formation in nonuniform mixtures. Obvious limitations of 1D models limit the reliability of their predictions, especially that of quantitative character. In view of this, it is important to mention some recent experimental results, which confirm, generally, the main conclusions of these calculations.

A series of experiments [3.36] was conducted to study critical conditions for propagation of explosion waves through reactivity gradients. Propagation of a detonation wave from a donor mixture through a gradient region to a less-reactive acceptor mixture was studied using hydrogen-air mixtures in a 174-mm tube. The length of the donor mixture, the width of the gradient region Δx, and the reactivity of acceptor mixture were varied in the tests. It was shown that a critical sensitivity gradient $(\Delta\lambda/\Delta x)^*$ ($\Delta\lambda$ is the difference in cell sizes between acceptor and donor mixtures) may be defined, which determines a possibility of detonation decay in the gradient region. Detonations decayed in the gradient region, in the cases of $(\Delta\lambda/\Delta x) > (\Delta\lambda/\Delta x)^*$. It was also found that the critical value of $(\Delta\lambda/\Delta x)^*$ depends significantly on the difference in energy densities of donor and acceptor mixtures. The more energetic the donor mixture was compared with the acceptor mixture, the sharper (greater $(\Delta\lambda/\Delta x)^*$) was the critical gradient for detonation decay. Extrapolation of the experimental results to the uniform energy density resulted in critical values of $(\Delta x/\Delta\lambda)^* \approx 10$. These experimental data, thus, appeared to be in accord, qualitatively, with the results of numerical calculations described earlier in this section. The critical values of the gradient for hydrogen-air mixtures appeared also to be in a reasonable quantitative agreement with the calculations.

Another aspect of the numerical and analytical predictions for the minimum size of a gradient region for detonation initiation concerns the effect of symmetry (initiation of spherical detonations). Recent results of turbulent jet initiation experiments [3.37] showed that the minimum requirement for initiation of spherical detonations by turbulent jet (in the absence of confining structure effects) may be expressed as $D_{jet} > 24\lambda$, where D_{jet} is the orifice size of the initiating jet. This is about 3 times as much as what should be expected for initiation of a planar wave (10λ) in accordance with results of numerical and analytical models.

These data support the results of theoretical analyses of main features of spontaneous onset of detonations in a sensitized mixture region. They show once more that some minimum size of the sensitized (or gradient) region is required for the onset of detonation. These results show, also, that the order of magnitude for the minimum size is about 10λ (λ corresponds to the surrounding mixture), and that this size can vary from several λ to several tenths of λ depending on particular conditions. In such a situation, a detonation onset criterion, which is aimed at describing the effect of scale with an accuracy better than an order of magnitude, should be primarily based on appropriate experimental correlations.

In the discussion presented here, the detonation cell size was used as a measure of mixture sensitivity. This allows scaling of DDT conditions found for different mixtures and compositions. The cell size data themselves are available for conditions typical of severe accidents. The data and corresponding interpolation methods are described in Appendix D. It should be noted, however, that the cell size cannot be considered as a fundamental mixture property. Its application as a scaling parameter should be validated experimentally. Fortunately, for mixtures typical of containment atmospheres (H_2-air, H_2-air-H_2O, H_2-air-CO_2 at normal and elevated initial temperatures), the detonation cell size has shown to be a reliable scaling parameter [3.38-3.42]. Corresponding details are given in Section 3.3.4.

3.3.3.3 L/λ-correlation (7λ criterion)

In order to formulate a criterion for the onset of detonations that describes the effect of scale, a definition of a *characteristic geometrical size* L of an enclosure is necessary. The size L should give a measure of the possible macroscopic size of a sensitized mixture where detonations might originate and develop. A requirement for this size to be large enough compared with the detonation cell size of the mixture can form the necessary detonation onset criterion. Originally [3.13, 3.32, 3.42, 3.43], such a criterion was formulated as $L > 7\lambda$, where L was defined as a characteristic (average) size of a room filled with combustible mixture (or the size of a mixture cloud). Experimental data generally showed a good agreement with $L > 7\lambda$ criterion over a wide range of scales and mixture compositions.

Despite a general agreement of the $L > 7\lambda$ criterion with experimental data, definitions for the characteristic size L used in References [3.13, 3.32, 3.42, and 3.43] were not always unambiguous, especially for practical applications. It was more or less established that good correlations were observed for rooms (or mixture clouds) with relatively small aspect ratios, where the size L could be easily defined as a sort of average of the corresponding geometrical sizes. An appropriate and clear definition of L for chains of connected rooms (or tubes with obstacles) was not derived in References [3.13, 3.32, 3.42, and 3.43]. Practical analyses of containment buildings showed that a system of connected rooms requires a special attention as the most typical geometry. In addition, a large amount of new experimental data was obtained recently, especially for DDT in obstructed channels. All these factors indicated that an additional analysis of the L/λ-correlation is of interest for practical applications.

The L/λ-correlation was reconsidered in Reference 3.44, in terms of a system of connected rooms. It was assumed that a characteristic size L_1 for a single room is the average size from two maximum room sizes. Such a definition showed a good correlation in earlier analyses, and provides a certain conservatism for rooms with large aspect ratios. We need to notice that the results of correlations are not very sensitive to the definition of the characteristic size of a single room. The average size, or the cubic root from the room volume, gives very close results for available experimental data.

Thus for single room it was assumed that

$$L_1 = (S + H)/2 , \tag{3.7}$$

where H and S are room height and length respectively (which are greater than room width W). It was suggested that if room 1 is connected with room 2 through some opening, the characteristic size L of the system of rooms 1 and 2 is defined by

$$L = L_1 + \alpha L_2 , \tag{3.8}$$

where L_1 and L_2 are characteristic sizes of room 1 and 2 respectively, and α is a parameter that describes the size of the opening between rooms. A large database on DDT conditions in obstructed channels and tubes can be used to find an appropriate definition for the parameter α. For long channels with repeated obstacles (which can be considered as a chain of rooms, all with characteristic sizes equal to L_1) one can obtain instead of Equation (3.8) the following form:

$$L = L_1 + \alpha(L_1 + \alpha(L_1 + \ldots)) , \tag{3.9}$$

or

$$L = L_1 + \alpha L . \tag{3.10}$$

Thus characteristic size for the channel with obstacles appeared to be given by

$$L = L_1/(1-\alpha) . \tag{3.11}$$

A comparison with experimental data for DDT in channels and tubes was made assuming different definitions for α, namely, $\alpha = (d/D)^{1/2}$, $\alpha = d/D$, and $\alpha = (d/D)^2$, where d is unobstructed passage, and D is tube diameter (or channel height $D = H$). It was found that the best correlation was observed for α defined as

$$\alpha = d/D . \tag{3.12}$$

Such a definition (Equations (3.7), (3.11), and (3.12)) for the characteristic size L is qualitatively in accord with observations that detonation onset is facilitated in obstructed channels with increase of d/D (decrease of blockage ratio) and with increase of obstacle spacing. Indeed, for the same D, L increases with increase of S and d/D. Moreover, the critical ratio L/λ for DDT appeared to be nearly constant for different configurations of obstacles and close to 7, as was suggested in the earlier studies [3.13, 3.32, 3.42, 3.43].

The characteristic size L of obstructed channels has clear geometrical interpretation, especially for cases of $S = H$. This observation is illustrated by Figure 3.3.3.3-1.

It should be noted that the definition for L (Equation (3.11)) has a singularity for $\alpha = 1$. This singularity leads to large increase of L for α close to unity (small BR). Such a singularity can be easily avoided by limiting the range of application of Equation (3.11) for the cases with large-enough values of BR, for example, BR > 0.1. In cases BR ≤ 0.1, the system of connected rooms can be considered as a single room with L defined by Equation (3.7).

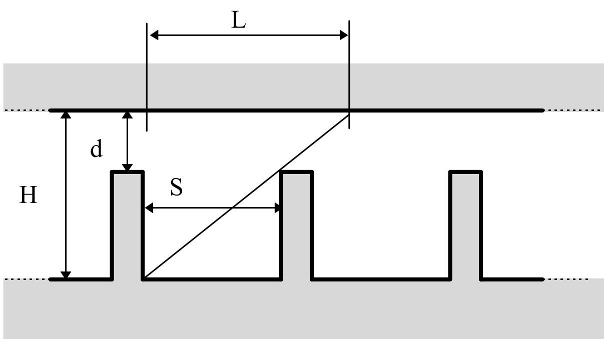

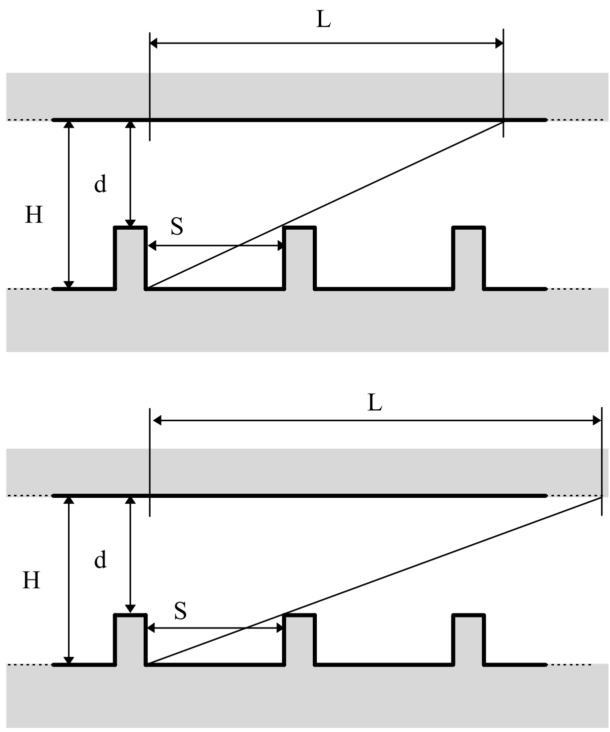

Figure 3.3.3.3-1 Graphical illustration of characteristic size L for channels with obstacles and its changes with blockage ratio.

3.3.3.4 Comparison of d > λ and L/λ Criteria

Both the minimum tube diameter and the L/λ criteria are based on comparison of characteristic geometrical sizes of an enclosure with the characteristic chemical length scale λ of the mixture. Applications of these criteria are limited by reliability of λ as a scaling parameter for a particular range of mixtures and initial conditions. This aspect should be verified first against an appropriate set of experimental data. The difference between these criteria is due to different definitions of characteristic geometrical sizes. In the $d > \lambda$ criterion, the minimum transverse size of unobstructed passage in a channel is required for onset of detonation. In the L/λ criterion, the minimum distance for detonation formation is required. These requirements, thus, do not contradict each other and may be considered as complimentary. The first approach ($d > \lambda$) is applicable to long channels with obstacles. The second one (L/λ), principally, allows us to address a wider range of typical geometrical configurations should an appropriate correlation be obtained.

3.3.4 Experimental Correlations for Detonation Onset Criteria

A considerable database has been accumulated in literature on limiting conditions for DDT. This database includes the McGill University small-scale tests on DDT [3.25-3.27], experiments in the FLAME Facility [3.15], BNL tests [3.11] and Whiteshell Laboratories (AECL) data [3.21]. Recently, large-scale DDT experiments with hydrogen-air, hydrogen-air-steam, and hydrogen-air-CO_2 mixtures were conducted at Russian Research Centre 'Kurchatov Institute' [3.13, 3.14, 3.38-3.40, 3.44, 3.45] in the RUT facility. Experiments were also made in MINIRUT experimental apparatus at scale 1:50 of RUT facility [3.45, 3.46]. New data on DDT conditions were also obtained in obstructed channels with transverse sizes 80, 174, 350, 520 mm [3.8, 3.9] for a wide range of hydrogen mixtures.

In this section, the detonation onset criteria are examined by comparison with this set of experimental data on DDT conditions.

3.3.4.1 Cell size as scaling parameter

Reliability of detonation cell size as a scaling parameter for detonation onset conditions can be estimated without any reference to DDT criteria. For that, critical values of λ for the onset of detonations should be compared in similar geometrical configurations and for different mixtures and scales. For hydrogen-air mixtures at relatively small scales, this comparison has already been done in the database [3.25-3.27] that summarizes a series of DDT experiments in tubes. It was also shown by results of DDT tests at BNL [3.11] for hydrogen-air-steam mixtures at initial temperatures up to 650 K.

A comparison of the critical λ values may be made also for a large range of scales and geometrical configurations on the basis of the RUT and MINIRUT tests, including

- hydrogen-air, hydrogen-air-steam, hydrogen-air-CO_2 mixtures at large scale;

- two typical geometrical configurations (obstructed channel and room); and

- two 50 times different scales.

Data of Tables 3.3.4.1-1 and 3.3.4.1-2 and Figures 3.3.4.1-1 and 3.3.4.1-2 show that the critical values of λ are similar for different mixtures and initial conditions at the same scale and geometrical configurations. The ratio of the critical λ-values is indeed close to the ratio of scales for tests with similar geometry.

It may be concluded that for the range of scales, mixtures, and initial conditions tested, detonation cell sizes can be used as a reliable scaling parameter for characterization of the detonation onset conditions.

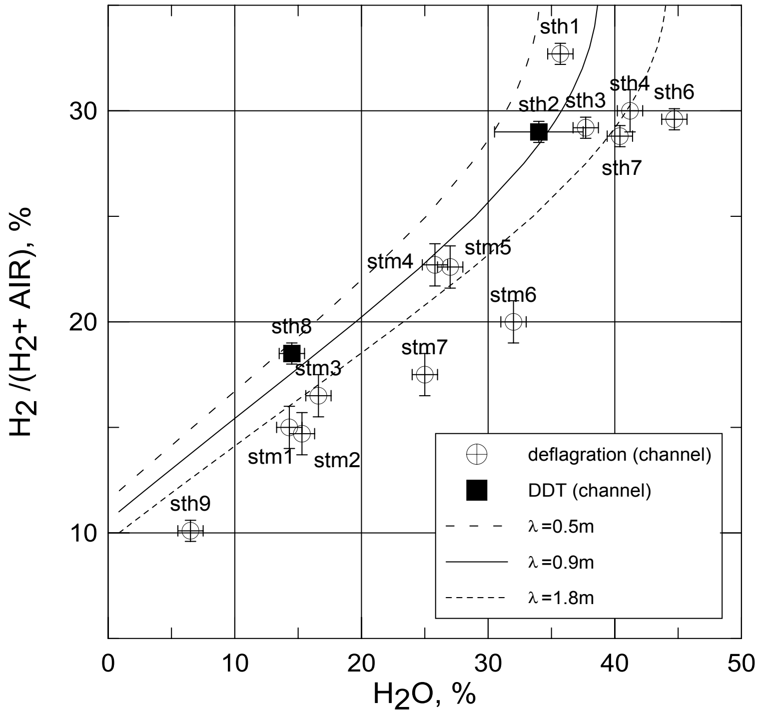

Figure 3.3.4.1-1 Combustion mode as a function of hydrogen (dry) and steam concentrations in an obstructed channel of the RUT Facility

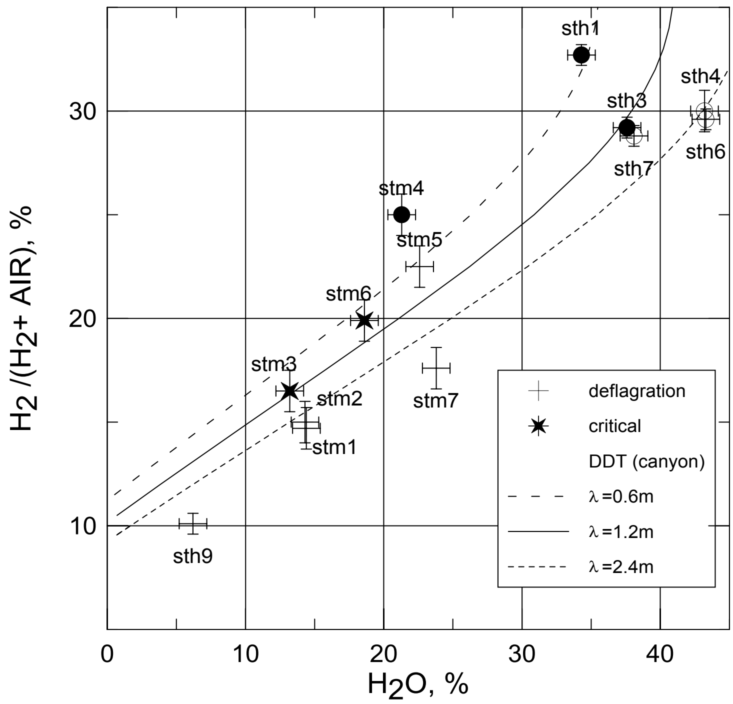

Figure 3.3.4.1-2 Combustion mode as a function of hydrogen (dry) and steam concentrations in a room (canyon) of the RUT Facility

Table 3.3.4.1-1 Critical values of λ for detonation onset at large scale (RUT facility)

Mixtures	Channel geometry	Room geometry
H_2/air at 285 K	-	≈1 m
H_2/air/H_2O at 375 K	≈ 0.9 m	≈1.2 m
H_2/air/CO_2 at 285 K	0.7 - 0.9 m	0.9 - 1.2 m

Table 3.3.4.1-2 Critical values of λ for detonation onset at two different scales and similar geometry

	RUT	MINIRUT (scale 1:50)	$\lambda_{RUT}/\lambda_{MINIRUT}$
	λ, mm		
Channel	900	18	50
Room	1200	21-25	48-57

3.3.4.2 L/λ-correlation (7λ criterion)

Characteristic geometrical sizes L and detonation cell widths of combustible mixtures are compared here for each particular case of deflagration and DDT. The characteristic sizes, L, were calculated for each case according to Equations (3.7), (3.8), (3.11), and (3.12). Detonation cell sizes were determined using data presented in Appendix D. Experimental data used for the L/λ-correlation are listed in Table 3.3.4.2-1

The summary of experimental results is presented in Figure 3.3.4.2-1. Data are marked with labels given in Table 3.3.4.2-1. Figure 3.3.4.2-1 shows combustion modes (DDT or deflagration) as a function of characteristic geometrical size L, and detonation cell width λ. A good correlation is observed for $L/\lambda \approx 7$ within the accuracy of the cell size data over a wide range of scales. The minimum ratio of $L/\lambda = 5.6$ for few cases of DDT can be found among the general borderline of $L/\lambda \approx 7$ in the correlation presented in Figure 3.3.4.2-1. This is just a 20% deviation, which is much smaller than inaccuracy of the cell size data.

It should be noted once more that such a correlation can be only considered as a necessary but not a sufficient condition for DDT. If 7λ criterion is not satisfied (over the 7λ line in Figure 3.3.4.2-1), detonation cannot be expected. In the opposite case (below the 7λ line in Figure 3.3.4.2-1), development of combustion process can result in both detonation and deflagration regimes. Data for channels with BR = 0.1 (d1 and t4 data labels) show an example that 7λ-criterion does not give a sufficient condition for DDT. Onset of detonations was observed in this case for ratios L/λ considerably higher than 7. Flame acceleration was inefficient with BR = 0.1, flames accelerated until the end of the channel, but did not reach a velocity high enough for DDT. For BR > 0.1, the necessary requirement for development of fast flames was satisfied, and DDT was observed in cases where the scale was large enough for onset of detonations ($L > 7\lambda$).

The data presented here show that quite a good L/λ-correlation can be obtained for a variety of different geometrical configurations. Probably, such a correlation can be further improved by using better definitions for characteristic size L. We need to note, however, that the accuracy of the cell size data for severe accident conditions is not as good as the agreement observed in Figure 3.3.4.2-1. As shown in Appendix D, average uncertainty in the cell size estimation is given by a factor of 1.5, and the maximum one can be more than a factor of 2. This should be taken into account in practical applications of the 7λ-criterion.

Table 3.3.4.2-1 Experimental data used in L/λ-correlation for onset of detonations

Data source	Label	Blockage ratio BR	Tube or channel size D (H), mm	Initial temperature T, K	Mixture type	Equivalence ratio ϕ
AECL [3.21]	a1	0.31	280	373	H_2/air/H_2O	
HTCF-BNL [3.11]	b1	0.43	273	300	H_2/air	<1
HTCF-BNL [3.11]	b2	0.43	273	500	H_2/air	<1
HTCF-BNL [3.11]	b3	0.43	273	650	H_2/air	<1
HTCF-BNL [3.11]	b4	0.43	273	400	H_2/air/H_2O	<1
HTCF-BNL [3.11]	b5	0.43	273	500	H_2/air/H_2O	<1
HTCF-BNL [3.11]	b6	0.43	273	650	H_2/air/H_2O	<1
CHANNEL-RRCKI [3.9]	c1	0.1	80	293	H_2/air	<1; >1
CHANNEL-RRCKI [3.9]	c2	0.3	80	293	H_2/air	<1; >1
CHANNEL-RRCKI [3.9]	c3	0.6	80	293	H_2/air	<1; >1
DRIVER-RRCKI [3.9]	d1	0.09	174	293	H_2/air	<1; >1
DRIVER-RRCKI [3.9]	d2	0.3	174	293	H_2/air	<1; >1
DRIVER-RRCKI [3.9]	d3	0.6	174	293	H_2/air	<1; >1
DRIVER-RRCKI [3.9]	d4	0.9	174	293	H_2/air	<1
FLAME-SNL [3.15]	f1	0.33	1830	293	H_2/air	<1
mini-FLAME-SNL [3.47]	f3	0.33	150	293	H_2/air	<1
FZK [3.9]	g1	0.6	350	293	H_2/air	<1; >1
FZK [3.9]	g2	0.6	350	293	$H_2/O_2/N_2$	1
FZK [3.9]	g3	0.3	350	293	H_2/air	1
FZK [3.9]	g6	0.6	350	293	H_2/air/CO_2	.5
FZK [3.9]	g7	0.6	350	293	H_2/air/CO_2	1
FZK [3.9]	g8	0.6	350	293	H_2/air/CO_2	2
FZK [3.9]	g9	0.6	350	293	H_2/air/CO_2	4
McGill [3.25]	m1	0.44	16 x 57 x 50	293	H_2/air	<1
McGill [3.25]	m2	0.44	16 x 57 x 100	293	H_2/air	<1
McGill [3.26]	m3	0.43	50	293	H_2, CH-fuels/air	<1
McGill [3.26]	m4	0.43	150	293	H_2, CH-fuels/air	<1
McGill [3.26]	m5	0.43	300	293	H_2, CH-fuels/air	<1
McGill [3.27]	m6	0.44	65 x 52 x 32	293	H_2, CH-fuels/air	<1
McGill [3.27]	m7	0.44	65 x 52 x 64	293	H_2, CH-fuels/air	<1
McGill [3.27]	m8	0.44	65 x 52 x 128	293	H_2, CH-fuels/air	<1
RUT-RRCKI [3.13]	r1	0.6	2250	293	H_2/air	<1
RUT-RRCKI [3.13]	r2	0.3	2250	293	H_2/air	<1
RUT-RRCKI [3.13]	r3	room	10.5 x 6 x 2.3 m	293	H_2/air	<1
RUT-RRCKI [3.14]	r4	room	10.5 x 6 x 2.3 m	375	H_2/air/H_2O	≤1
RUT-RRCKI [3.14]	r5	0.3	2250	375	H_2/air/H_2O	≤1
RUT-RRCKI [3.40]	r6	0.3	2250	293	H_2/air/CO_2	<1
RUT-RRCKI [3.40]	r7	room	10.5 x 6 x 2.3 m	293	H_2/air/CO_2	<1
RUT-RRCKI [3.45]	ri	room	15 x 6 x 2.3 m	293	H_2 -injection	≤1

continued . . .

Table 3.3.4.2-1 (concluded)

Data source	Label	Blockage ratio BR	Tube or channel size *D* (*H*), mm	Initial temperature *T*, K	Mixture type	Equivalence ratio ϕ
HDT-SNL [3.12]	s1	0.6	406	383	H_2/air	>1
HDT-SNL [3.12]	s2	0.3	406	383	H_2/air/H_2O	>1
TORPEDO-RRCKI [3.9]	t1	0.6	520	293	H_2/air	<1; >1
TORPEDO-RRCKI [3.9]	t3	0.3	520	293	H_2/air	<1; >1
TORPEDO-RRCKI [3.9]	t4	0.1	520	293	H_2/air	<1; >1
mini-RUT-RRCKI [3.44]	v1	0.3	46	293	H_2/air	<1
mini-RUT-RRCKI [3.44]	v2	room	210 x 120 x 50	293	H_2/air	<1

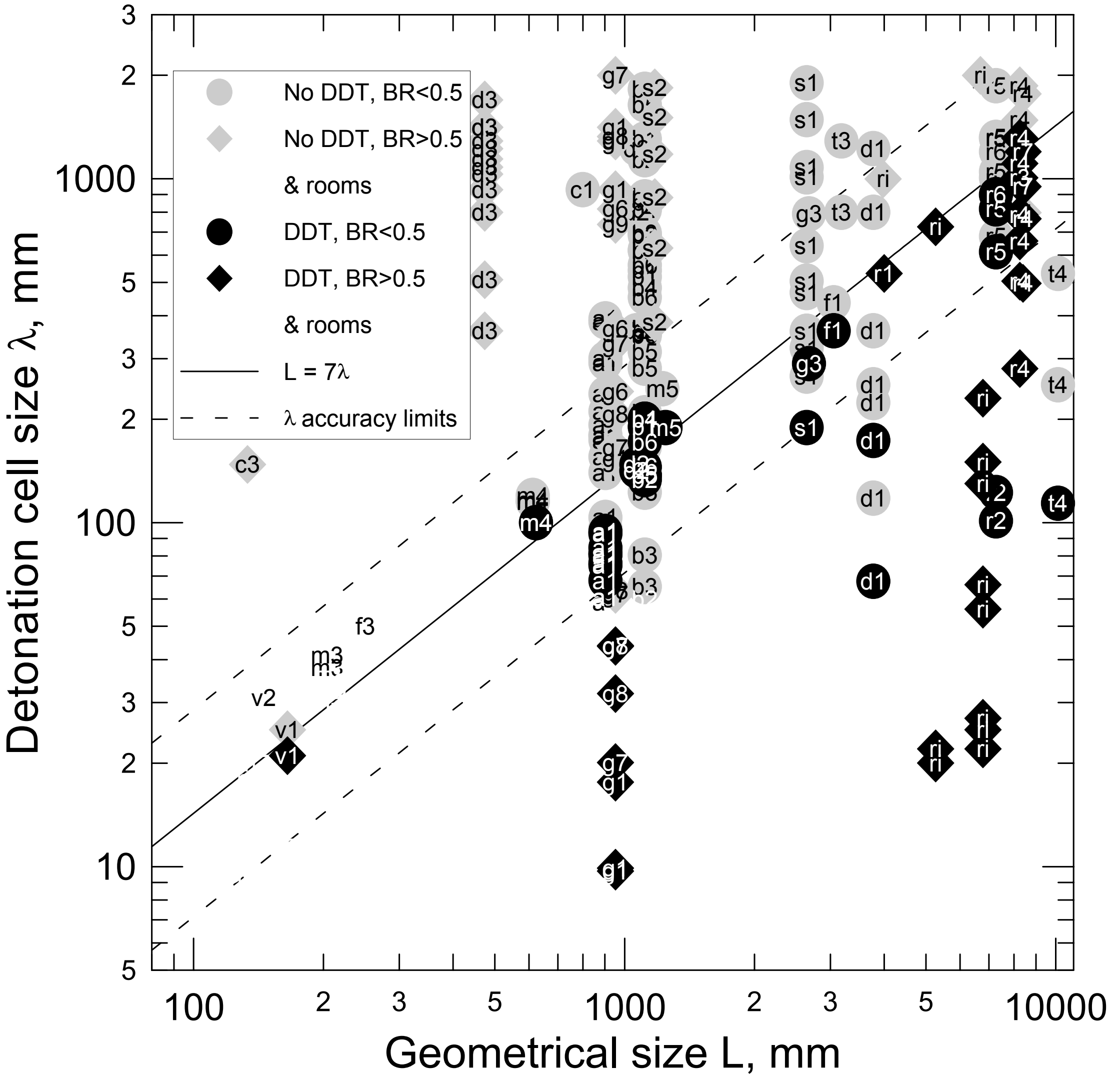

Figure 3.3.4.2-1 ***L/λ*-correlation for onset of detonations**

3.3.4.3 *Correlations for turbulent jet initiation*

The initiation of detonations by a turbulent jet of combustion products represents one type of DDT phenomena. This initiation mode can occur when combustion of a gaseous mixture in a confined chamber with a venting orifice results in the injection of combustion products' jet through the orifice into another mixture volume outside the chamber (see Figure 3.3.4.3-1). It was shown first by Knystautas et al. in 1979 [3.48] that such a jet is able to initiate detonation in the surrounding mixture in cases the jet gas velocity and the jet size are large enough. Since that time, a number of studies were conducted to determine critical conditions for turbulent jet initiation of detonation [3.37, 3.48-3.56]. Correlations of the jet orifice size d_0 and detonation cell size λ of the surrounding mixture were usually used to characterize the critical conditions. A considerable spread of the critical d_0/λ values from about 10 to more than 60 can be found in these studies.

It has been indicated in many studies [3.37, 3.49-3.51, 3.53-3.56] that the onset of detonation is usually induced or influenced by confining structures. A limited number of observations have been made that show direct initiation of detonation in the turbulent jet of combustion products [3.37, 3.51, 3.55, 3.56]. As suggested in Reference [3.37], the cases when initiation process is dominated by interaction with confining structures are rather cases of DDT but not true cases of the turbulent jet initiation. The turbulent jet plays a role of a strong ignition source, and detonation occurs at a later stage of combustion. The jet orifice size is not a single characteristic scale in these cases, and correlations in terms of d_0/λ are not appropriate to characterize the critical conditions.

To extract experimental data that correspond to true cases of turbulent jet initiation, one can consider the results of the tests under nearly unconfined conditions. These are tests where the combustible mixture was confined with only a thin plastic bag [3.37, 3.51, 3.54, 3.55] and tests where the size of the experimental chamber was large enough compared with the jet orifice size d_0 [3.55]. A correlation for critical conditions of the turbulent jet initiation, based on these data is presented in Figure 3.3.4.3-2. Figure 3.3.4.3-2 shows that minimum jet orifice size d_0 for onset of detonations in the jet can be estimated in the range from 14λ to 24λ.

As mentioned in Section 3.3.3, the minimum scale requirement for the onset of detonation in the spherical initiation mode is more severe than that in the planar case, and the difference can be described approximately by a factor of 3. If detonation onset is observed near the rigid wall or near the ground surface, it is possible to assume that an explosion wave develops initially as a planar wave. In the truly unconfined conditions (far from physical boundaries), only a spherical wave can be initially formed. This is the case for detonation formation directly in the turbulent jet. It may be suggested that the difference in experimental correlations $L/\lambda > 7$ and $d_0/\lambda > (14 \div 24)$ can be attributed mainly to the different (planar or spherical) initiation modes.

If one considers combustion processes in a system of connected rooms, the scenario of jet initiation is, principally, possible. An initiating jet can be formed in the connection between two compartments with the size d_0. Because d_0 is always smaller than the characteristic room size L, the requirement for direct initiation in the jet $d_0 > (14 \div 24)\lambda$ appears to be much less demanding than that for DDT ($L > 7\lambda$). In this situation, DDT should be considered as a more probable event. However, if condition $d_0 > (14 \div 24)\lambda$ is satisfied, there is a high probability that detonation will be initiated next to the connection. Such an estimate of DDT location can be important for safety analysis because very high local loads are typical of DDT events.

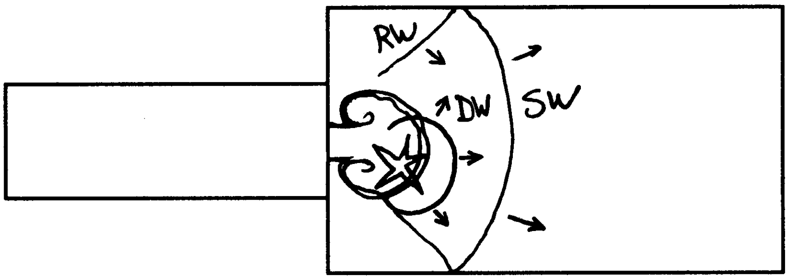

Figure 3.3.4.3-1 Schematic illustration of turbulent jet initiation of detonation. Jet of combustion products enters from the left chamber through an orifice to the right chamber. A detonation wave (DW) can be originated in the products and reactants mixing region.

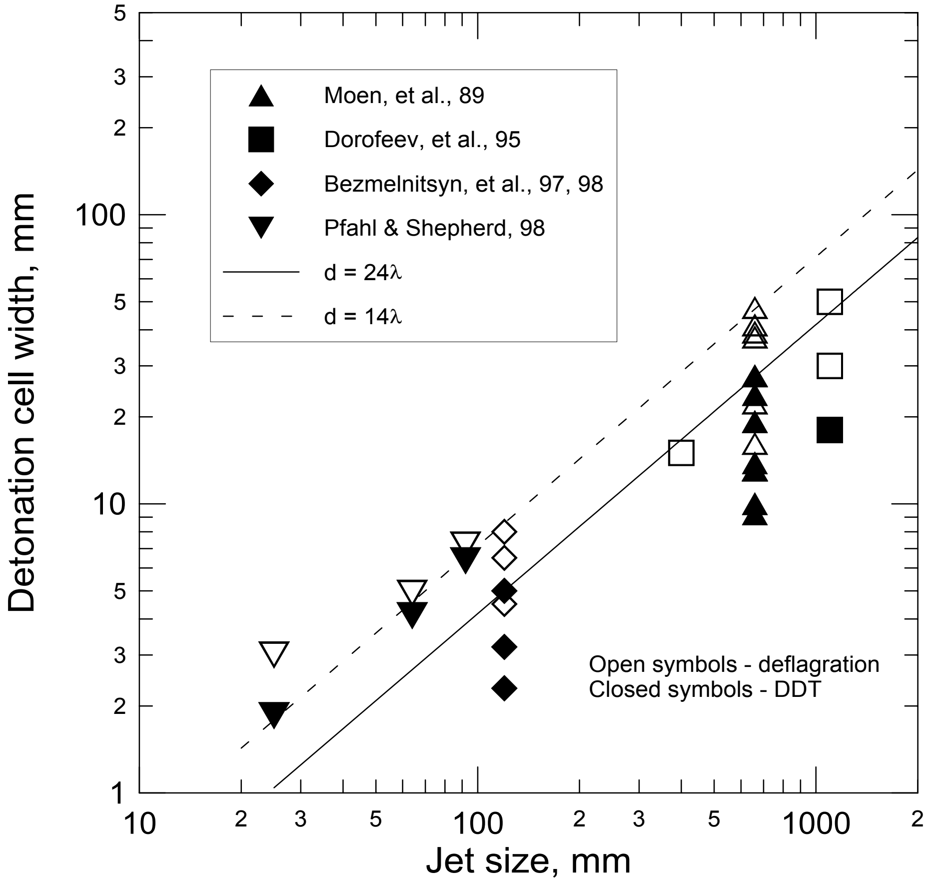

Figure 3.3.4.3-2 Correlation for initiation of spherical detonations by a turbulent jet of combustion products. Data are taken from References [3.37, 3.51, and 3.54-3.56].

3.3.5 Applications of DDT Criteria and Corresponding Uncertainties

First of all, we need to emphasize once more that all DDT criteria considered in this report may be used as necessary conditions only. They give a sign that DDT can principally be expected under certain conditions and scale. They do not show, however, that DDT will necessarily occur, if these criteria are satisfied. The most important point for practical application is that DDT should not be expected, if one of these criteria is not satisfied. The necessary DDT criteria, thus, are appropriate for conservative estimates of the possibility of DDT. The term "conservative" here means that an analysis based on necessary but not sufficient conditions is conservative since it can indicate a possibility that DDT can occur in some cases when DDT cannot actually occur because of factors that are not considered in the analysis. The level of such a conservatism can be reduced if several DDT criteria are used simultaneously. At the same time, it should be emphasized that these are empirical criteria. They are based on the currently available set of data, and it is possible that they will be revised in future as more information becomes available.

DDT criteria impose limitations on different phases and aspects of the combustion process. Among the criteria considered in this report, σ, d/λ, L/λ, and d_0/λ correlations are the most readily available for nuclear safety applications. Application and uncertainties of σ-criterion for flame acceleration were discussed in Section 3.2.4. Here, the detonation onset criteria will be discussed.

3.3.5.1 d/λ correlation (minimum tube diameter criterion)

Application of this criterion is appropriate for relatively long channels. In the case of rooms, or connected compartments with large blockage ratios, the d/λ-criterion can result in significantly overconservative estimates. Inaccuracy of the cell size data should be taken into account in practical applications.

3.3.5.2 L/λ correlation (7λ criterion)

This criterion was formulated in order to address different geometrical configurations typical of a containment building. For each compartment of a containment, a characteristic size L should be determined. In most cases of particular geometrical configurations, Equations (3.7) to (3.12) give a guideline for determination of L.

It should be noted, however, that actual geometry of a containment does not always permit a clear definition of L as it was used in Equations (3.7) to (3.12). Some necessary amendments are given below. In cases of some difficulties with determination of L, the general approach should be to use the maximum L value from a number of choices.

In a typical situation of a system of connected rooms, some rooms can be connected to several others. Characteristic size L of the room 1 connected to rooms 2 , . . . , n can be calculated according to an extended version of Equation (3.8):

$$L = L_1 + \alpha_2 L_2 + \ldots + \alpha_n L_n , \tag{3.13}$$

where $\alpha_2, \ldots \alpha_n$ are parameters that describe sizes of connections between rooms. Such a way to account for neighbouring rooms is only important for large-enough open connections between rooms.

In some situations, parameter α cannot be defined directly as $\alpha = d/D$. Several possible ways to replace Equation (3.12) can be suggested:

$$\alpha = (L_1 s/V_1)^{1/2} ; \tag{3.14}$$

$$\alpha = (s/6/\Phi)^{1/2}, \tag{3.15}$$

where s is the area of connection to a neighbouring room, V_l is total volume of the room, and $\boldsymbol{\Phi}$ is total area of all room walls, including open connections. Equations (3.14) and (3.15) are written using parameters that can be easily defined in a containment.

Inaccuracies of determination of L for some cases define the first type of uncertainty in application of L/λ correlation. The range of this uncertainty can be estimated using difference in L values calculated using different available options for each particular case. Generally, this is certainly lower by a factor of 2, which defines the accuracy of the cell size data.

A second type of uncertainty is defined by the accuracy of the cell size data. As shown in Appendix D, average uncertainty in the cell size estimation for nuclear safety applications is given by a factor of 1.5, and the maximum one can be more than a factor of 2. This inaccuracy should be taken into account by using a correction factor for λ values for L/λcorrelation. If λ is determined using interpolation methods presented in Appendix D, the cell size values reduced by a factor of 1.5 to 2 should be used in L/λ correlations. This is necessary because far interpolations and even extrapolations of the cell size data are unavoidable in applications. A possibility to use directly the cell size values can be considered on case-by-case basis if mixture compositions and initial conditions are close to the range of reliable experimental data (see Appendix D).

A third type of uncertainty is connected with applications of L/λ correlation for volumes with characteristic size exceeding 10 to 15 m (the range given is due to inaccuracy of λ). The problem is that no detonations were observed in experiments with a cell size of more than 2 m. This is the maximum reported λ-value, which was estimated in HDT Facility tests at the Sandia National Laboratories from spacing of a transverse wave for a single-spin detonation. Thus any extrapolation of the cell size values beyond $\lambda \approx 2$ m is questionable. It does not mean, however, that L/λ correlation is useless for large compartments with $L > 10$ to 15 m (e.g., dome part of a containment). Application of this correlation gives a conclusion that DDT is possible in such compartments for all mixtures with $\lambda < 2$m. Possibility of DDT in mixtures less sensitive than those with $\lambda \approx 2$m is uncertain.

In view of this uncertainty, it may be suggested that the possibility of effective flame acceleration should be the main interest for large compartments. Namely, σ-correlations can be applied. If effective flame acceleration is impossible (weak mixture), fast flames cannot be developed and DDT is impossible as well, disregarding the value of λ. In the opposite case, development of fast explosion regimes, including detonations, cannot be excluded.

3.3.5.3 d_0/λ-correlation (turbulent jet initiation)

As mentioned in the previous section, DDT in a given compartment is a much more probable event compared with the turbulent jet initiation. Thus, d/λ and L/λ should be used first. Critical conditions for turbulent jet initiation can be useful to identify locations where the onset of detonation can be expected.

3.3.5.4 Combination of σ- and L/λ-correlations

An example of the combined application of σ and L/λ correlations is presented in Figure 3.3.5.4-1 for hydrogen-air steam mixtures at 375 K and 1 atm initial pressure. Conservative estimates were used for limits of flame acceleration (the minimum σ*-values). The DDT border is shown as λ = 2 m curve. This means that inside this border, DDT is possible in rooms with $L > 7*2/1.5 \approx 10$ m. It should be emphasized that DDT limits depend on scale, whereas flame acceleration limits (σ criterion) do not.

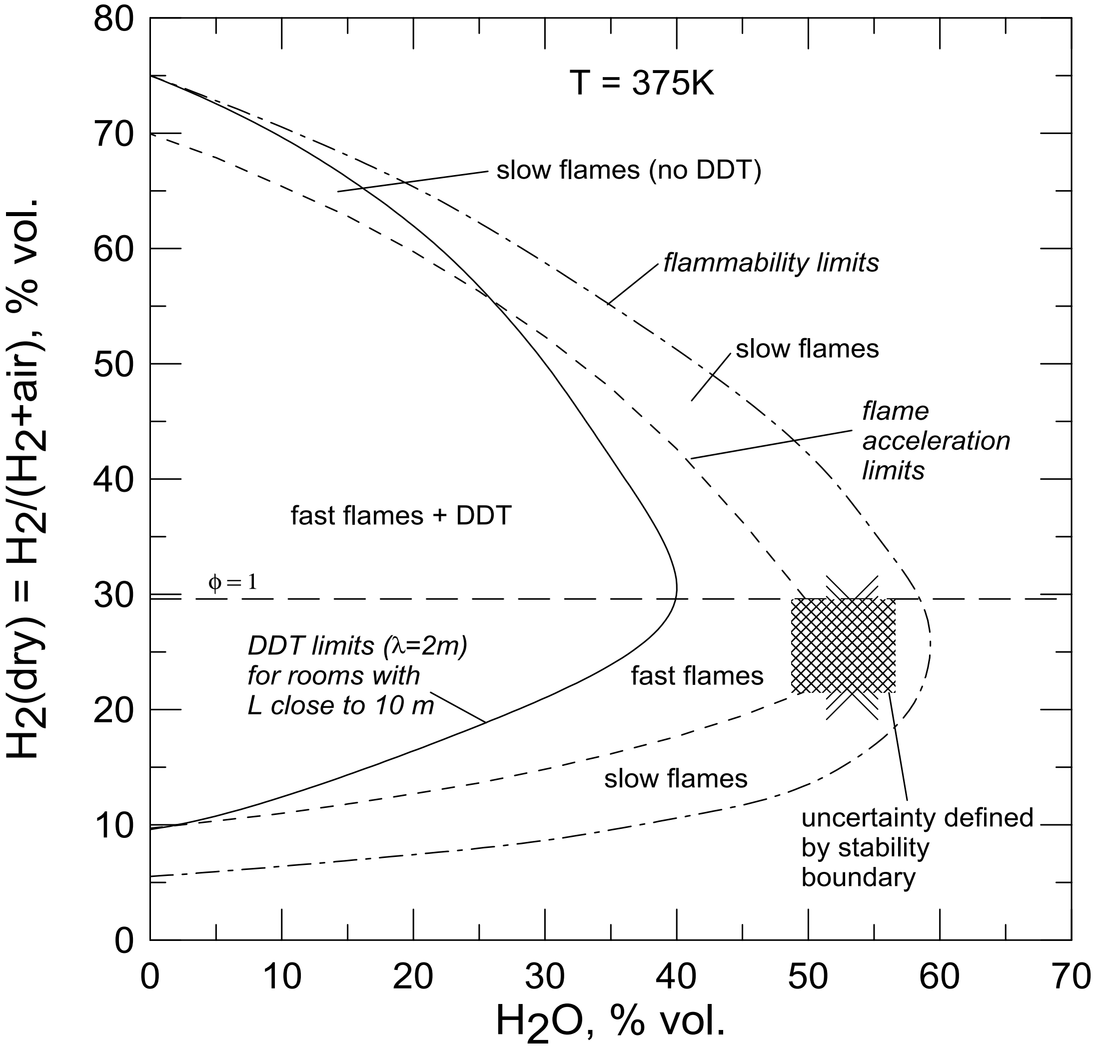

Figure 3.3.5.4-1 Limits and possible regimes of combustion for hydrogen-air-steam mixtures at T = 375 K and p = 1 atm

3.3.5.5 Application of L/λ correlation in non-uniform mixtures

Concentration gradients can be expected in a containment as a result of the processes of hydrogen injection and mixing. In the case that a concentration gradient exists in a compartment or combustible cloud, it is difficult to directly apply the criteria for detonation onset that are based on detonation cell size λ. It is necessary, at least, to define what λ value from the range defined by the concentration distribution should be used as the representative chemical length scale.

The most conservative assumption is to use the minimum λ, which corresponds to the most-sensitive mixture composition. At the same time, it is a highest probability that a detonation is originated in the most-sensitive part of the mixture (minimum cell size). To classify a detonation as a global event for the given compartment or cloud, the detonation should be transmitted then to the less-sensitive part. This possibility, as explained in Section 3.3.3, depends mainly on the value of λ in the insensitive part of mixture surrounding the detonation origin.

To resolve this conflict an approximation can be suggested that some average cell size should be compared with characteristic size L of the compartment (cloud) to estimate wheter a detonation is possible as a global event. Because of non-linear behaviour of the cell size function on concentration (see Appendix D), λ of average composition $<C>$ is usually smaller than the average cell size $<\lambda>$. Thus the use of $\lambda(<C>)$ gives more conservative estimates for L/λ criterion. In many cases, the average composition is the only information available from distribution calculations (e. g., from lumped-parameter codes).

It should be emphasized that the use of $\lambda(<C>)$ for L/λ criterion gives only a global estimate. If L appears to be less than $7\lambda(<C>)$, it does not mean that detonation cannot be expected locally, somewhere inside the compartment (cloud), where mixture is more sensitive. To make more detailed estimations, information on composition distribution is required.

If such information is available, one can consider the following logical scheme. Assuming that detonation is formed already inside a small volume with a characteristic size X_1 with a sensitive composition C_1, one can test whether the detonation survives propagation to the distance X_2 with less-sensitive composition C_2. A schematic of such a problem for planar case, which will be considered first, is shown in Figure 3.3.5.5-1

According to the results [3.35], the possibility of detonation transition to location X_2 is defined dominantly by the length of the gradient $L \approx X_2$, and the value of cell size at location X_2: $L > A\lambda(C_2)$. Factor A depends on the energy density difference between mixtures C_1 and C_2. For constant energy density it is close to 7 used in the L/λ correlation. If this difference is described through CJ detonation velocities D_1 and D_2, experimental data for lean hydrogen air mixtures [3.36] suggest that

$$\log(A) \propto \cdot D_1^2/D_2^2\,, \tag{3.16}$$

If one assumes for simplicity that C_1 and C_2 represent concentrations of a limiting component, then $D_1^2/D_2^2 \approx C_1/C_2$. According to Equation (3.16), for a given C_2, $\log(L)$ decreases linearly with C_1 as shown in Figure 3.3.5.5-1. Point C in Figure 3.3.5.5-1 corresponds to the critical value of L_C for detonation formation at location X_2.

Point E in Figure 3.3.5.5-1 gives an estimation of critical L from the cell size of the least-sensitive mixture ($L_E = 7\lambda(C_2)$), without taking into account the energy density difference (underconservative estimate). Point A corresponds to the critical L_A defined by the minimum λ ($L_A = 7\lambda(C_1)$) and gives an overconservative estimate. Point A should be always lower than point C since the minimum L_A defined by this point is a fraction of L_C value for point C.

Point B is defined as $L_B = 7\lambda(<C>)$. If the function $log(\lambda) = f(C)$ is concave, what is generally true for hydrogen-air-steam mixtures, point B is lower than C, giving a conservative estimate for L/λ correlation. The same is not always true for point D ($L_D = 7(<\lambda>)$). Thus the above consideration gives an explanation of why the use of $\lambda(<C>)$ for L/λ correlation should give a conservative estimate.

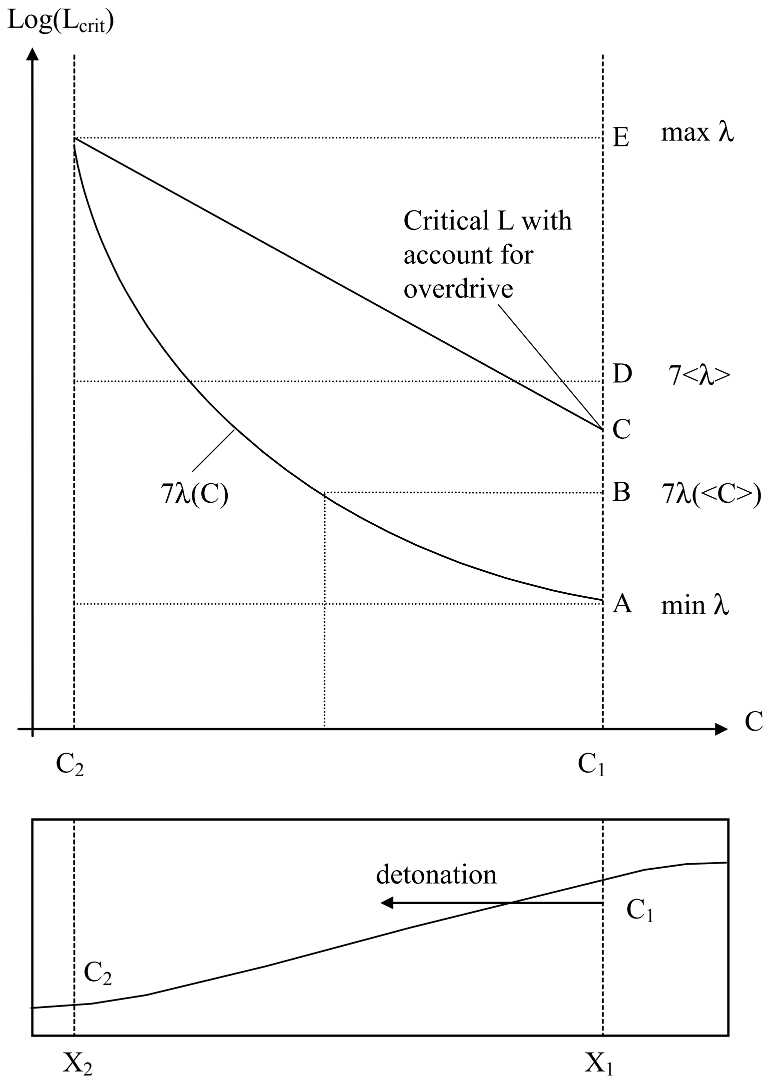

Figure 3.3.5.5-1 Schematic illustration of different options to estimate minimum cloud size (critical gradient) for the possibility of detonation in a location X_2 in that cloud.

In the non-planar cases of detonation wave formation, the above speculations can be also applicable, but factor A is expected to be greater than 7, as mentioned in Section 3.2.3.2. This value gives an additional conservatism in applications of the criterion $L > 7(\langle\lambda\rangle)$.

Thus two possible approximate solutions can be suggested for application of L/λ correlation for non-uniform cases. The first one makes use of the characteristic size L of a compartment (mixture cloud) and the cell size of the average composition. The criterion $L > 7\lambda(\langle C\rangle)$ should give an estimate of the possibility of global detonations in the compartment. If detailed distribution of components is unknown and significant gradients can be expected, the possibility of local detonations in a part of the compartment (cloud) cannot be estimated with this criterion.

This approach was applied in large-scale experiments on dynamic hydrogen injection and ignition in the RUT Facility [3.45] and showed good results. Corresponding data (labelled "ri") are shown in Figure 3.3.4.2-1.

The second solution implies that concentration distribution is known. One can start from the cloud boundary with determination of L $(\approx V^{1/3})$ and $\langle\lambda\rangle$, and test the criterion $L/\lambda(\langle C\rangle)$ for the cloud. If it is not satisfied, a more sensitive part of the cloud can be enveloped, new values of L and $\lambda(\langle C\rangle)$ can be determined, and the criterion can be tested again. This procedure can be repeated going into smaller and more sensitive cloud parts. If at a certain stage the 7λ criterion appears to be satisfied, this means that detonation is principally possible, locally, inside this part of the mixture. Such a procedure that gives indications of the possibility of local detonations should be considered, thus, as more conservative compared with the first solution.

It should be noted that these solutions for non-uniform mixtures can be applied only as estimates. Although they are based on the DDT correlations for uniform cases and on experimental data on detonation behaviour in non-uniform mixtures (lean hydrogen-air at normal initial temperature and pressure), no direct experiments are available to verify them in detail.

3.4 Summary

An overview of criteria for FA and DDT has been presented in this chapter. These criteria address one of the important practical problems, namely, what type of combustion might be expected: slow flames, fast flames, or detonations. It was shown that boundaries separating various flame regimes depend not only on the composition of the mixture, but also on thermodynamic state, geometrical configuration, and on the physical size or scale of an enclosure.

It is important to note that only a number of empirical necessary conditions for FA and DDT have been formulated up to the present. They are based on the currently available set of data, and are the subject of ongoing research.

One of these conditions states that FA is only possible in mixtures having large-enough expansion ratio $\sigma > \sigma^*$ (see details in Section 3.2). The requirement of large-enough σ is the necessary but not a sufficient condition for development of fast combustion regimes. A sufficiently long flame path and/or favourable geometrical configuration promoting flame folding and stretching should be present in order that the flame can actually accelerate to high velocities. If the flame has accelerated to velocities of about the speed of sound in combustion products, the conditions for spontaneous formation of detonation can be reached.

The second important set of the necessary conditions states that detonation may only occur if the physical size L the compartment containing mixture is sufficiently large compared to the chemical length scale that characterizes the sensitivity of the mixture. The usual choice of the chemical length scale is the detonation cell size λ. The necessary criteria for DDT described in Section 3.3 are expressed in a form of $L > \alpha\lambda$. The value of the constant α depends on the particular geometrical configuration and on the definition of the characteristic geometrical size L (see details in Section 3.3).

Combined application of FA and DDT criteria enable a more refined evaluation of possible combustion regimes than was previously possible for severe accidents in nuclear power plants. At the same time there are uncertainties, which are described in Sections 3.2.4 and 3.3.4. These uncertainties should be taken into account in practical applications of the criteria for FA and DDT.

3.5 References

3.1. V. S. Babkin, A. Ya. Vykhristuk, V. N. Krivulin, et al., *Archivum Combustionis,* Vol. 4, No 4, 1984, 321.

3.2. I. O. Moen, J. H. S. Lee, B. H. Hjertager, K. Fuhre and R. K. Eckhov, Pressure Development due to Turbulent Flame Acceleration in Large-Scale Methane-Air Explosions, *Combustion and Flame*, Vol. 47, 1982, 31-52.

3.3. I. O. Moen, M. Donato, R. Knystautas, J. H. S. Lee and H. Gr. Wagner, In: *AIAA Progress in Astronautics and Aeronautics*, Vol. 75, 1981, 31.

3.4. B. H. Hjertager, M. Bjørkhaug and K. Fuhre, Gas Explosion Experiments in 1:33 and 1:5 Scale Offshore Separator and Compressor Modules using Stoichiometric Homogeneous Fuel/Air Clouds, *Journal of Loss Prevention in Processes Industries*, Vol. 1, 1988, 197-205.

3.5. C. A. Catlin and D. M. Johnson, Experimental Scaling of the Flame Acceleration Phase of an Explosion by Changing Fuel Gas Reactivity, *Combustion and Flame*, Vol. 88, 1992, 15-27.

3.6. R. G. Abdel-Gayed and D. Bradley, Criteria for Turbulent Propagation Limits of Premixed Flames, *Combustion and Flame*, Vol. 62, 1985, 61-68.

3.7. R. G. Abdel-Gayed, D. Bradley, M. H. Hamid and M. Lawes, Lewis Number Effects on Turbulent Burning Velocity, *20th Symposium International on Combustion*. The Combustion Institute, Pittsburgh, 1984, 505-512.

3.8. S. B. Dorofeev, M. S. Kuznetsov, V. I. Alekseev, A. A. Efimenko, A. V. Bezmelnitsyn, Yu. G. Yankin and W. Breitung, Effect of Scale and Mixture Properties on Behavior of Turbulent Flames in Obstructed Areas, Preprint IAE-6127/3, RRC "Kurchatov Institute" Report FZKA-6268, Forschungszentrum Karlsruhe, 1999.

3.9. M. S. Kuznetsov, V. I. Alekseev, A. V. Bezmelnitsyn, W. Breitung, S. B. Dorofeev, I. D. Matsukov, A Veser and Yu. G. Yankin, Effect of Obstacle Geometry on Behavior of Turbulent Flames. Preprint IAE-6137/3, RRC "Kurchatov Institute", Report FZKA-6328, Forschungszentrum Karlsruhe, 1999.

3.10. S. B. Dorofeev, M. S. Kuznetsov, V. I. Alekseev, A. A. Efimenko and W. Breitung, Evaluation of Limits for Effective Flame Acceleration in Hydrogen Mixtures. Preprint IAE-6150/3, RRC "Kurchatov Institute" Report FZKA-6349, Forschungszentrum Karlsruhe, 1999.

3.11. G. Ciccarelly, J. Boccio, T. Ginsberg, C. Finfrock, L. Gerlach, H. Tagava and A. Malliakos, The Effect of Initial Temperature on Flame Acceleration and Deflagration-to-Detonation Transition Phenomenon, NUREG/CR-6509, BNL-NUREG-52515, 1998.

3.12. M. P. Sherman, M. Berman and R. F. Beyer, Experimental Investigation of Pressure and Blockage Effects on Combustion Limits in H_2-air-steam Mixtures, Sandia National Laboratories Report No. SAND91-0252, 1993.

3.13. S. B. Dorofeev, V. P. Sidorov, A. E. Dvoinishnikov and W. Breitung, Deflagration to Detonation transition in Large Confined Volume of Lean Hydrogen-Air Mixtures, *Combustion and Flame* Vol. 104, 1996, 95–110.

3.14. S. B. Dorofeev, V. P. Sidorov, A. E. Dvoinishnikov, A. Denkevits, A. Efimenko and A. Lelyakin, Large Scale Hydrogen-Air-Steam DDT Experiments in the RUT Facility. Test Series 1996. Report RRC KI 80-05/16, RRC "Kurchatov Institute", 1997.

3.15. M. S. Sherman, S. Tieszen, and W. Benedick, The Effect of Obstacles and Transverse Venting on Flame Acceleration and Transition to Detonation for Hydrogen-Air Mixtures at Large Scale, NUREG/CR-5275, SAND 85-1264, 1989.

3.16. P. Clavin, Dynamic Behavior of Premixed Flame Fronts in Laminar and Turbulent Flows, *Progress in Energy and Combustion Sciences*, Vol. 11, 1985, 1-59.

3.17. J. E. Shepherd and J. H. S. Lee, On the Transition from Deflagration to Detonation. In:: Major Research Topics of Combustion, M. Y. Hussaini, A. Kumar, R. G. Voit Eds. Springer Verlag, Berlin, 1991.

3.18. M. Berman, A Critical Review of Recent Large-Scale Experiments on Hydrogen-Air Detonations, *Nuclear Science and Engineering*, Vol. 93, 1986, 321-347.

3.19. C. M. Guirao, R. Knystautas and J. H. S. Lee, A Summary of Hydrogen-Air Detonations for Reactor Safety, Report NUREG/CR-4961, Sandia National Laboratories/McGill University, 1989.

3.20. O. Peraldi, R. Knystautas and J. H. S. Lee, Criteria for Transition to Detonation in Tubes, *21st Symposium International on Combustion,* The Combustion Institute, Pittsburgh, PA, 1986, 1629-1637.

3.21. C. K. Chan and W. A. Dewit, Deflagration to Detonation Transition in End Gases, *26th International Symposium on Combustion*, The Combustion Institute, Pittsburgh, PA, 1996, 2679-2684.

3.22. C. K. Chan, Collision of a Shock Wave with Obstacle in a Combustible Mixture, *Combustion and Flame* 100, 1995, 341-348.

3.23. B. E. Gelfand, O. E. Popov, S. P. Medvedev, S. V. Khomok, A. Yu. Kusharin and G. L. Agafonov, Selfignition of Hydrogen-oxygen Mixtures at High Pressure, In: CD-ROM *Proceedings of 21th International Symposium on Shock Waves*, paper 2400, 1997.

3.24. B. Gelfand, S. Khomik, S. Medvedev, A. Polenov, A. Bartenev, W. Breitung and A. Veser, A. Investigation of Hydrogen-air Fast Flame Propagation and DDT in Tube with Multidimensional Endplates *Proceedings of the Colloquium on Gas, Vapor, Hybrid and Fuel-Air Explosions*, Schaumburg, IL, USA, 21-25 September, 1998, 434-455.

3.25. A. Teodorczyk, J. H. S. Lee, R. Knystautas, Photographic Studies of the Structure and Propagation Mechanisms of Quasi-Detonations in a Rough Tube, In: *AIAA Progress in Astroanautics and Aeronautics*, Vol. 133, 1990, 233-240.

3.26. J. H. Lee, R. Knystautas and C. K. Chan, Turbulent Flame Propagation in Obstacle-filled Tubes, *20th Symposium International on Combustion.* The Combustion Institute, Pittsburgh, PA, 1984, 1663-1672.

3.27. A. Teodorczyc, J. H. S. Lee and R. Knystautas, Propagation Mechanisms of Quasi-detonations, *22nd Symposium International on Combustion.* The Combustion Institute, Pittsburgh, PA, 1988, 1723-1731.

3.28. Ya. B. Zel'dovich, B. E. Gelfand, S. A. Tsyganov, S. M. Frolov and A. N. Polenov, Concentration and Temperature Non-Uniformities (CTN) of Combustible Mixtures as a Reason of Pressure Generation, In: *AIAA Progress in Astronautics and Aeronautics* (A. L. Kuhl, Ed.), Vol. 114, 1988, 99-123.

3.29. M. Short and J. W. Dold, Corrections to Zel'dovich's Spontaneous Flame and the Onset of Detonation via Nonuniform Preheating, In: AIAA *Progress in Astronautics and Aeronautics* (A. L. Kuhl, Ed.), Vol. 154, 1993, 59-74.

3.30. J. W. Dold, M. Short, J. F. Clarke and N. Nikiforakis, Accumulating Sequence of Ignitions from a Propagating Pulse, *Combustion and Flame*, Vol. 100, 1995, 475-473.

3.31. S. B. Dorofeev, A. S. Kochurko and B. B. Chaivanov, Detonation Onset Conditions in Spatially Nonuniform Combustible Mixtures, *Sixteenth Symposium (International) on Loss Prevention and Safety Promotion in the Processes Industries,* Oslo, Vol. 4, 1989, 22-1 - 22-19.

3.32. S. B. Dorofeev, A. A. Efimenko, A. S. Kochurko and B. B. Chaivanov, Evaluation of the Hydrogen Explosions Hazard, *Nuclear Engineering and Design,* Vol. 148, 1994, 305-316.

3.33. S. B. Dorofeev, A. A. Efimenko and A. S. Kochurko, Numerical Study of Detonation Self-initiation Conditions, *Proceedings of 15th International Colloquium on Dynamics of Explosions and Reactive Systems*, Boulder, Colorado, 1995, 425-428.

3.34. A. M. Khokhlov, E. S. Oran and J. C. Wheeler, A Theory of DDT in Unconfined Flames, *Combustion and Flame,* Vol. 108, 1997, 503-517.

3.35. S. I. Kryuchkov, S. B. Dorofeev and A. A. Efimenko, Critical Conditions for Detonation Propagation through Mixture with Decreasing Reaction Rate, *26th International Symposium on Combustion*, The Combustion Institute, Pittsburgh, 1996, 2965-2972.

3.36. M. S. Kuznetsov, V. I. Alekseev, S. B. Dorofeev, I. D. Matsukov and J. L. Boccio, Detonation Propagation, Decay, and Reinitiation in Nonuniform Gaseous Mixtures, *27th Symposium International on Combustion*. The Combustion Institute, Pittsburgh, 1998, 2241-2247.

3.37. A. V. Bezmelnitsyn, S. B. Dorofeev and Yu. G. Yankin, Direct Comparison of Detonation Initiation by Turbulent Jet under Confined and Unconfined Conditions, *Proceedings of 16th International Colloquium on Dynamics of Explosions and Reactive Systems*, Cracow, Poland, 1997, 222-225.

3.38. V. P. Sidorov and S. B. Dorofeev, Large-Scale Experiments and Scaling of DDT Conditions in Hydrogen-Air-Steam Mixtures - an Overview, *Proceedings of the Workshop on Severe Accident Research in Japan* (SARJ-97) JAERI-Conf 98-009, 1998, 162-182.

3.39. V. P. Sidorov and S. B. Dorofeev, Influence of Initial Temperature, Dilution and Scale on DDT Conditions in Hydrogen-air mixtures, *Arhivum Combustionis*, Vol. 18, No 1-4, 1998, 87-103.

3.40. V. P. Sidorov, M. S. Kuznetsov, I. D. Matsukov, V. I. Alekseev, A. V. Denkevits and S. B. Dorofeev, Large Scale DDT and Detonation Transmission Experiments with Hydrogen Containing Mixtures in the RUT Facility. Test Series 1998. Report RRC "Kurchatov Institute" RRC KI 80-05/17, April 1999.

3.41. S. B. Dorofeev, Effect of Scale on the Onset of Detonations, *Proceedings of 7th International Conference on Numerical Combustion.* York, UK, 1998, 24-25.

3.42. S. B. Dorofeev, V. P. Sidorov, W. Breitung and A. S. Kotchourko, Large-scale Combustion Tests in the RUT Facility: Experimental Study, Numerical Simulations and Analysis on Turbulent Deflagrations and DDT, *Transactions of 14th International Conference on Structural Mechanics in Reactor Technology,* Lyon, France, Vol. 10, 1997, 275-283.

3.43. S. B. Dorofeev, Turbulent Combustion and DDT Events as an Upper Bound for Hydrogen Mitigation Techniques, OECD/NEA/CSNI Workshop on the Implementation of Hydrogen Mitigation Techniques, Winnipeg, Manitoba, Canada, 1996, AECL-11762, NEA/CSNI/R(96)8, 415-433.

3.44. S. B. Dorofeev, V. P. Sidorov, M. S. Kuznetsov, I. D. Matsukov and V. I. Alekseev, Effect of Scale on the Onset of Detonations, In: *CDROM Proceedings of 17th International Colloquium on Dynamics of Explosions and Reactive Systems*, Heidelberg, Germany, 1999, ISBN 3-932217-01-2.

3.45. I. D. Matsukov, M. S. Kuznetsov, V. I. Alekseev and S. B. Dorofeev, Photographic Study of Transition from Fast Deflagrations to Detonations, *22nd International Symposium on Shock Waves*, London, UK, 1999, 370-375.

3.46. S. B. Dorofeev, V. P. Sidorov and W. Breitung, Explosions Resulted from Accidental Release and Ignition of Hydrogen at Dynamic Conditions, *Pre-prints of the 2nd International Specialist Meeting on Fuel-Air Explosions*, Bergen, Norway, 1996, 3.36-3.48.

3.47. M. P. Sherman, S. R. Tieszen and W. B. Benedick, Sandia National Laboratories Report No. SAND89-0859, 1989.

3.48. R. Knystautas, J. H. Lee, I. O. Moen and H. G. Wagner, Direct Initiation of Spherical Detonation by a Hot Turbulent Gas Jet, *17th Symposium International on Combustion*, The Combustion Institute, Pittsburgh, PA, 1979, 1235-1242.

3.49. M. Schildknecht, W. Geiger and M. Stock, Flame Propagation an Pressure Buildup in a Free Gas-Air mixture Due to Jet Ignition, In *AIAA Progress in Astronautics and Aeronautics* (A.L. Kuhl, Ed.), Vol. 94, 1985, 474-490.

3.50. I. O. Moen, D. Bjerketvedt, A. Jenssen and P. A. Thibault, Transition to Detonation in a Large Fuel-Air Cloud, *Combustion and Flame* Vol. 61, 1985, 285-291.

3.51. I. O. Moen, D. Bjerketvedt, T. Engenbretsen and A. Jenssen, Transition to Detonation in a Flame Jet, *Combustion and Flame* Vol. 75, 1989, 297-308.

3.52. F. Carnasciali, J. H. S. Lee, R. Knystautas and F. Fineschi, Turbulent Jet Initiation of Detonation, *Combustion and Flame* Vol. 84, 1991, 170-180.

3.53. S. B. Dorofeev, A. V. Bezmelnitsyn, V. P. Sidorov, Yu. G. Yankin and I. D. Matsukov, Turbulent Jet Initiation of Detonation in Hydrogen-Air Mixtures, Proc. *14th International Colloquium on Dynamics of Explosions and Reactive Systems*, University of Coimbra, Coimbra, Vol. 2, 1993, D2.4.1-D2.4.10.

3.54. S. B. Dorofeev, V. P. Sidorov, A. E. Dvoinishnikov and A. V. Bezmelnitsyn, Transition to Detonation in Large Confined and Unconfined Fuel-air Clouds, *Proceedings of 15th Int. Colloquium on the Dynamics of Explosions and Reactive Systems*, Boulder, CO, 1995, 421-425.

3.55. A. V. Bezmelnitsyn, Experimental Study of Conditions for Detonation Initiation by a Jet of Combustion Products. Ph.D. dissertation, RRC “Kurchatov Institute”, Moscow, 1998.

3.56. U. J. Pfahl and J. E. Shepherd, Jet Initiation of Deflagration and Detonation in Stoichiometric H_2-O_2-N_2 Mixtures, GALCIT Report FM 99-1. California Institute of Technology, Pasadena, CA USA, 1988.